



Technische Universität München
Fakultät für Medizin

**The role of juvenile murine hippocampal synaptic plasticity and
microvasculature in brain injury after partial-brain radiation**

Hengyi Fan

Vollständiger Abdruck der von der Fakultät für Medizin der Technischen Universität München zur Erlangung des akademischen Grades eines

Doktors der Medizin

genehmigten Dissertation.

Vorsitzender: Prof. Dr. Jürgen Schlegel

Prüfer*innen der Dissertation: 1. Prof. Dr. Gabriele Multhoff
2. apl. Prof. Dr. Gerhard Rammes
3. Priv.-Doz. Dr. Jens Gempt

Die Dissertation wurde am 18.05.2021 bei der Technischen Universität München eingereicht und durch die Fakultät für Medizin am 07.12.2021 angenommen.

Table of Contents

Table of Contents.....	2
List of Figures	5
List of abbreviations.....	6
1. Introduction.....	9
1.1 Radiation-induced brain injury.....	9
1.1.1 Epidemiology.....	9
1.1.2 Classification	11
1.1.3 Prevention/Amelioration strategies	12
1.1.3.1 Lithium	13
1.1.3.2 Memantine.....	14
1.1.3.3 Donepezil	15
1.1.3.4 Antioxidants	16
1.1.3.5 Anti-inflammatory agents	17
1.1.3.6 Hippocampal avoidance approaches	18
1.2 Pathophysiology of radiation-induced brain injury	20
1.2.1 Radiation-induced vascular changes.....	22
1.2.2 Blood brain barrier (BBB) disruption.....	23
1.2.3 Loss of hippocampal neurogenesis.....	24
1.2.4 NPC dysfunction	25
1.2.5 Astrocyte senescence	26
1.2.6 Dendritic morphological and functional change of mature neurons	27
1.3 Hippocampus	29
1.3.1 Introduction	29
1.3.2 Role of hippocampus in radiation-induced CI.....	31

1.4	Aim of study	33
2.	Materials and Methods	35
2.1	Materials	35
2.1.1	Equipment.....	35
2.1.2	Software	35
2.1.3	Consumables.....	36
2.1.4	Chemicals	37
2.1.5	Antibodies	39
2.1.6	Buffers and solutions	39
2.2	Methods	40
2.2.1	Animal care and partial-brain radiation (PBRT) procedure	40
2.2.2	Randomization and blinding	42
2.2.3	Protocol for the assessment of the effect of PBRT on juvenile murine unilateral hippocampal synaptic plasticity and microvascular	42
2.2.4	Immunohistochemistry (IHC).....	43
2.2.5	Electrophysiological field recording.....	44
2.2.6	Hippocampi staining and clearing using EMOVI	46
2.2.6.1	EMOVI sample preparation.....	46
2.2.6.2	Digestion	47
2.2.6.3	Antibody staining	48
2.2.6.4	Dehydration and clearing.....	48
2.2.6.5	Image acquisition	49
2.2.6.6	Data processing and analysis	49
2.2.7	Statistical analysis	50
3.	Results	51
3.1	PBRT of the left hemisphere of mouse brains	51
3.2	PBRT inhibits LTP in the CA1 region of hippocampal slices 3 days after radiation.....	53
3.3	LTP in irradiated hippocampal slices was blocked by different PBRT regimen, while unaffected in the contralateral hippocampus	55

3.4	LTP in juvenile mice remained inhibited at 10 weeks after irradiation	60
3.5	Radiation affects LTP dose- and time-dependent.....	64
3.6	Effects of different dose regimen on body weight of juvenile mice.....	68
3.7	Quantitative hippocampus microvasculature network analysis.....	69
4.	Discussion.....	74
5.	Summary	81
6.	References.....	82
7.	Appendix.....	94
8.	Acknowledgements.....	95
9.	Curriculum Vitae.....	98

List of Figures

Figure 1. The percentage of patients developing radiation-induced CI as a function of time after fractionated WBRT.....	11
Figure 2. Schematic illustration of the anatomic location of the DG of the hippocampus within the rodent brain.....	20
Figure 3. Pathophysiology mechanisms of radiation-induced brain injury.....	22
Figure 4. Schematic representation of radiation compromising dendritic spine density through excessive accumulation of glutamate in the hippocampus.....	28
Figure 5. Sagittal view of the adult mouse brain focusing on two neurogenic niches where NSCs resides in the V-SVZ of the LV and DG of the hippocampus.....	30
Figure 6. (A) Picture of the SARRP used in this study. (B) and (C) CT scan for mouse body.....	41
Figure 7. Schematic of PBRT mice project design.....	43
Figure 8. (A) Anesthetized mice treated with PRRT 20Gy after 10 weeks. (B) Left and right intact hippocampi were removed with a razor blade from the intact mouse brain.....	47
Figure 9. Irradiation protocol and γ -H2A.X-stained section.....	52
Figure 10. PBRT inhibits CA1-LTP of irradiated hippocampal slices.....	54
Figure 11. After 5 weeks recovery from PBRT, LTP in hippocampal slices is inhibited dose-dependently.....	58
Figure 12. LTP in juvenile mice except 2Gy PBRT remained inhibited 10 weeks after irradiation.....	63
Figure 13. Fractionated 4+4Gy and 20Gy high single dose radiation inhibit LTP.....	67
Figure 14. The histograms of effects of different doses on mice body weight.....	68
Figure 15. Efficient tissue clearing and multi-organ volumetric imaging.....	70
Figure 16. Quantitative vessel network analysis reveals significant loss in hippocampus following targeted PBRT.....	72

List of abbreviations

ACSF	Artificial cerebrospinal fluid
BBB	Blood brain barrier
CA	Cornu Ammonis
CI	Cognitive impairment
CNS	Central nervous system
DG	Dentate gyrus
DSB	Double-strand break repair
EMOVI	Efficient tissue clearing and multi-organ volumetric imaging
fEPSPs	field excitatory postsynaptic potentials
HA-WBRT	Hippocampal avoidance-whole brain radiation
HFS	High frequency stimulation
IHC	Immunohistochemistry
LTP	Long-term potentiation
LTD	Long-term depression
LV	Lateral ventricle

NMDA	N-methyl-D-aspartate
NMDARs	N-methyl-D-aspartate receptors
NPCs	Neural progenitor cells
NSCs	Neural stem cells
PBRT	partial-brain radiation
PBS	Phosphate buffer saline
PFC	Prefrontal cortex pathway
PPAR	Peroxisome proliferator-activated
QOL	Quality of life
RAS	Renin–angiotensin system
RT	Radiotherapy
SASP	Senescence-associated secretory phenotype
SARRP	Small-animal radiation research platform
SRS	Stereotactic radiosurgery
SGZ	Subgranular zone
SVZ	Subventricular zone

V-SVZ

Ventricular-subventricular zone

WBRT

Whole-brain radiation

1. Introduction

1.1 Radiation-induced brain injury

1.1.1 Epidemiology

Serving as a frontline treatment modality for primary intracranial tumors and intracranial metastases, postoperative irradiation followed by chemotherapy prolongs survival, increases longevity and improves quality of life.(Hochberg & Pruitt, 1980; Keime-Guibert et al., 2007) Whole-brain radiation (WBRT) is the standard of care to improve intracranial control following resection of brain metastasis (Kocher et al., 2011) and is used as a prophylactic therapy in patients with small cell lung cancer with a high risk for brain metastases.(Slotman et al., 2007) Each year approximately 100,000 patients receive brain radiotherapy (RT) in the US, however, 50%-90% of these patients who survive for more than 6 months suffer from a radiation-induced cognitive impairment (CI).(Crossen et al., 1994; Giovagnoli & Boiardi, 1994; Greene-Schloesser et al., 2013; Greene-Schloesser & Robbins, 2012; Johannesen et al., 2003; Meyers & Brown, 2006; Wilke et al., 2018) CI mainly involves hippocampus related functions, such as learning, memory, spatial information synthesis, and the risk of cognitive dysfunction caused by RT mainly occurs in patients who survive for a longer time period.(Greene-Schloesser

et al., 2012; Roman & Sperduto, 1995) (Figure 1) CI appears as early as 3-4 months after RT with predominantly memory and executive function failures.(P. D. Brown et al., 2016; Chang et al., 2009; J. Li et al., 2007) With the improvement of treatment planning of intracranial tumors, the survival time of patients is significantly prolonged, and the probability of CI after RT is increased.(Chang et al., 2009) Currently, few studies focus on CI following brain radiation and reported prevalence variations range between 19% to 90%. These findings are most likely due to heterogeneous patient cohorts but also due to tumor-related variables and patient demographics. (Laack & Brown, 2004; Meyers et al., 2004; van Kessel et al., 2017) The decline in quality of life (QOL) caused by cognitive dysfunctions after RT has a significant negative impact on the patient and the entire society. Eliminating late side effects caused by RT will significantly improve the QOL of patients and reduce the burden on the society.(Liu et al., 2009) Therefore, it is of great importance to study the pathogenic mechanisms and treatment options for CI after brain RT.

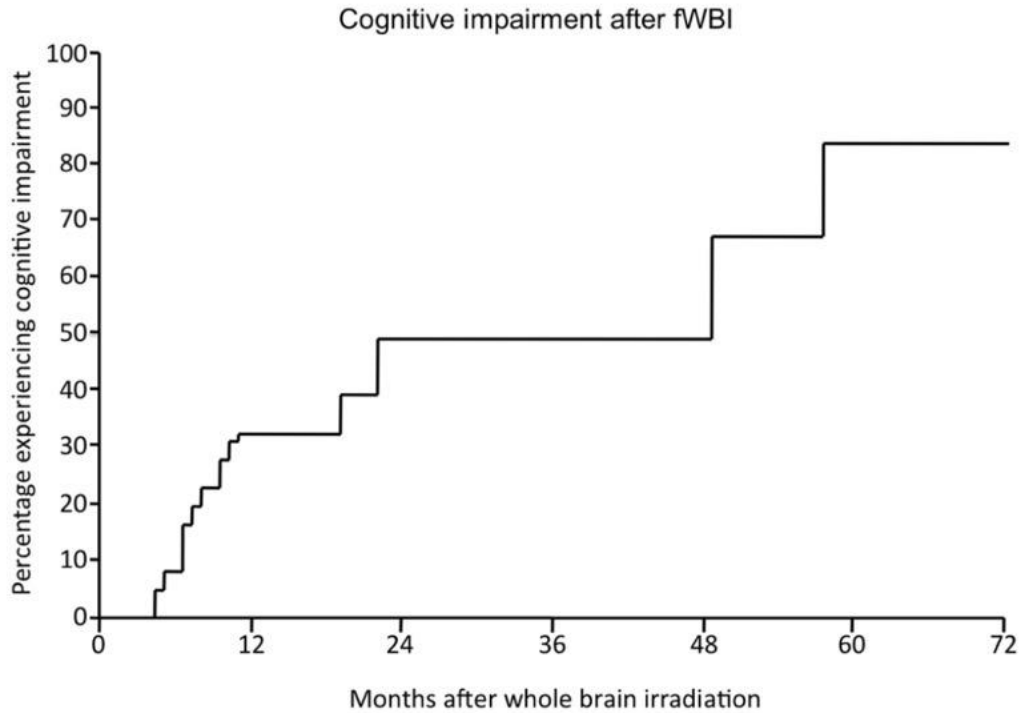


Figure 1. The percentage of patients developing radiation-induced CI as a function of time after fractionated WBRT.(Greene-Schloesser et al., 2012)

1.1.2 Classification

According to the time between the start of RT and the onset of side effects, radiation-induced brain injury are traditionally categorized into acute, early-delayed, and late-delayed side effects.(Greene-Schloesser et al., 2012; Hopewell & Wright, 1970; Locksmith & Powers, 1968; Sheline et al., 1980; Tofilon & Fike, 2000;

Walker et al., 2014) Acute and early-delayed injuries appear days to 6 months after RT, the symptoms are reversible or recovery occurs spontaneously. On the contrary, late-delayed injury manifests at least half a year after RT and these deficits are irreversible and progressive. While acute injury arises from edema, headaches, drowsiness, the early-delayed phase is characterized by transient demyelination, somnolence, attention deficits, and short-term memory loss. Late-delayed injury is characterized by white matter necrosis, vascular abnormalities, and more permanent demyelination, gliosis, and lasting cognitive dysfunction.

1.1.3 Prevention/Amelioration strategies

There are different strategies to minimize radiation-induced neurotoxicity, which include enhancement of neuronal survival and hippocampal neurogenesis, inhibition of neurotoxic microenvironment. Drugs such as memantine, anti-inflammatory agents that are routinely used in other neurological disorders have recently been repurposed to ameliorate CI.

1.1.3.1 Lithium

Lithium, a well-known mood stabilizer, is now considered as a potent candidate which supports prevention and recovery after different types of cranial injury, including WBRT.(Contestabile et al., 2013; H. Li et al., 2011; Q. Li et al., 2010; Malaterre et al., 2012) It has also been used in routine clinical practice for 60 years.(Fountoulakis et al., 2005) In lithium pre-treated animal models, lithium could increase proliferation of hippocampal neural progenitor cells (NPC) and rescue radiation-induced cell cycle arrest.(Zanni, Di Martino, et al., 2015) It regulates adult hippocampal NPC development through the activation of Wnt canonical pathway by inhibition of glycogen synthase kinase 3.(Wexler et al., 2008) Moreover, it induces neurogenesis, protects hippocampal neurons from radiation-induced apoptosis and ameliorates functional deficits after radiation to the immature mouse brain.(Huo et al., 2012; Yazlovitskaya et al., 2006) Preclinical studies also indicate that it might be beneficial for adult and young patients to restore cognitive functions after RT.(Malaterre et al., 2012; Zanni, Zhou, et al., 2015) More recently, Zanni et al. suggested that lithium administration following radiation needs to be given intermittently to induce NPC proliferation and to allow them to differentiate upon drug discontinuation.(Zanni et al., 2021)

1.1.3.2 Memantine

Glutamate represents a crucial excitatory amino acid neurotransmitter in cortical and hippocampal neurons.(Orrego & Villanueva, 1993) Glutamate accumulation and excessive stimulation of glutamate receptors induce intracellular calcium overload, which eventually results in excitotoxicity. Many pathological conditions in CNS, such as stroke, epilepsy and brain injury are related to this mechanism. As a noncompetitive, low-affinity, open-channel antagonist of N-methyl-D-aspartate (NMDA) type glutamate receptors (NMDARs), memantine is involved in learning and memory by modulating neuronal transmission and synaptic plasticity. Specifically, it also has been approved to be applied in dementia and Alzheimer's disease.(Attia et al., 2014) In several preclinical models of brain radiation(Duman et al., 2018; D. Zhang et al., 2018) and phase III trials(P. D. Brown et al., 2020; P. D. Brown et al., 2013), memantine better preserves cognitive functions and improves symptoms reported by patients. A possible protective mechanism of memantine pre-administration is the prevention of radiation-induced toxicities at hippocampal excitatory synapses.(Duman et al., 2018)

1.1.3.3 Donepezil

CI is also characterized by a decreased activity of choline acetyltransferase, which result in lower levels of acetylcholine and an impaired neuronal signaling.(Malouf & Birks, 2004) As a reversible noncompetitive inhibitor of acetylcholinesterase, donepezil improves cognitive functions in patients with moderate to severe Alzheimer's dementia,(Birks & Harvey, 2018; Scarpini et al., 2003) Parkinson's disease,(Leroi et al., 2004) and traumatic brain injury(L. Zhang et al., 2004) by increasing cholinergic-dependent neural communication.(Seltzer, 2007) Furthermore, it improves cerebral perfusion in brain cognitive processing region(L. Zhang et al., 2004) and is also highly selective for acetylcholine esterase and well tolerated(Wilcock et al., 2002) in healthy young(Gron et al., 2005) and older adults.(FitzGerald et al., 2008) A phase III clinical trial suggests treatment with a daily dose of donepezil for irradiated brain tumor survivors could lead to modest improvements in several cognitive functions, especially among patients with greater pretreatment impairments after RT.(Rapp et al., 2015)

1.1.3.4 Antioxidants

The production of reactive oxygen species (ROS) including peroxides, superoxide, hydroxyl radicals, and singlet oxygen (Hayyan et al., 2016) play a crucial role in radiation-induced brain injury. Neurons are specifically susceptible to ROS due to their increased unsaturated fatty acid contents and higher lipid peroxidation in response to radiation. (Turnquist et al., 2020) Aydemir et al. reported that both plasma and tissue levels of total antioxidant status significantly changed in favor of antioxidant activity after administration of the antioxidant drug quercetin. (Kale et al., 2018) As a natural body hormone which regulates the circadian rhythm, melatonin is a promising antioxidant and anti-inflammatory agent. It has been shown that melatonin could ameliorate radiation-induced oxidative organ damage in rats. (Sener et al., 2003) The mechanisms of radioprotection and radiosensitization of melatonin could not only be attributed to neutralize various types of free radicals produced by radiation or pro-oxidant enzymes, but also to the protective effect on NSCs against lipopolysaccharide-induced inflammation, (Song et al., 2015) thereby mitigating radiation injury. (Amini et al., 2019; Farhood et al., 2019) Besides, animal studies confirmed that melatonin reduces apoptosis and upregulates the NSC marker nestin in the ventricular-subventricular zone (V-SVZ) in irradiated rat brains. (Naseri et al., 2017) Another radioprotective and antioxidant

agent is the natural non-flavonoid polyphenolic resveratrol, which plays an important role in the protection of hippocampal neurons from oxidative stress by activating Sirtuin 1 to stop radiation-induced apoptosis.(J. Li et al., 2014; Truong et al., 2018) It also has neuroprotective effects on irradiated NSCs residing in the juvenile hippocampus, which enables it to be a potential supplement to Hippocampal avoidance-WBRT (HA-WBRT).(Prager et al., 2016) The mechanisms underlying resveratrol's protective effect against oxidative neuronal death are attributed to selectively induce the expression of mitochondrial superoxide dismutase, and thereby subsequently reduce mitochondrial oxidative stress and damage.(Fukui et al., 2010; Fukui & Zhu, 2010) Moreover, a natural analog and a metabolite of resveratrol could inhibit the increase of glutamate following radiation-induced neuronal cell death and ROS formation.(Son et al., 2013)

1.1.3.5 Anti-inflammatory agents

Many preclinical studies provide theoretical basis for the administration of anti-inflammatory-based interventions to inhibit or ameliorate late radiation-induced brain injury, including CI.(Hong et al., 1995; W. H. Lee et al., 2010; Monje et al., 2002; Rola et al., 2004; Schindler et al., 2008) Both renin–angiotensin system (RAS)

inhibitors and peroxisome proliferator-activated (PPAR) agonists prevent radiation-induced CI in animal models by effectively reducing inflammatory pathway cascades including NF- κ B and AP-1 and activating neuroprotective as well as anti-inflammatory pathways in the central nervous system (CNS), respectively. (Bright et al., 2008; T. C. Lee et al., 2012; Ramanan et al., 2010; Robbins et al., 2010; Schnegg et al., 2013; Stahel et al., 2008; W. Zhao et al., 2007) For instance, mice treated with PPAR agonist fenofibrate after WBRT lead to an increased number of hippocampal neurons and a decreased microglial activation. (Ramanan et al., 2009) RAS blockers ramipril could prevent CI in young adult male rats before, during, and after radiation. (T. C. Lee et al., 2012) Additionally, it has shown that combined atorvastatin and ramipril interact synergistically to potently and selectively ameliorate radiation-induced impairment of hippocampal neurogenesis. (Jenrow et al., 2011)

1.1.3.6 Hippocampal avoidance approaches

The hippocampus plays a key role in learning and memory. Radiation dose to the hippocampus neuro regenerative zone correlates with cognitive toxicity since NPC of the dentate gyrus (DG) (Figure 2) are particularly vulnerable to

radiation.(Haldbo-Classsen et al., 2020; Kotecha & Hall, 2020; Redmond et al., 2013)

Reducing the radiation dose to the hippocampus during WBRT has been clinically considered as an effective strategy to mitigate the neurocognitive deficits. HA-WBRT techniques have demonstrated the ability to reduce the mean dose to the hippocampus by at least 80%, while providing acceptable coverage and dose homogeneity to the remaining brain tissue.(P. D. Brown et al., 2020; Oskan et al., 2014) To avoid toxic effects induced by WBRT, patients with brain metastases are frequently treated with stereotactic radiosurgery (SRS)(P. D. Brown et al., 2017; Kocher et al., 2011) or HA-WBRT plus memantine to preserve cognitive function.(P. D. Brown et al., 2020) There are several studies indicating that patients with few brain metastases are better protected against cognitive deficiencies by using SRS(P. D. Brown et al., 2017; P. D. Brown et al., 2016; Chang et al., 2009) or HA-WBRT.(Gondi, Tolakanahalli, et al., 2010; Gondi, Tome, et al., 2010; Gutierrez et al., 2007; Harth et al., 2013; Kim et al., 2016; Kundapur et al., 2015; Oehlke et al., 2015; Oskan et al., 2014; Prokic et al., 2013; R. Zhao et al., 2017) Another phase II clinical trial reported that intensity-modulated radiotherapy (IMRT) can also be used to avoid damage on the hippocampal neural stem-cell compartment during HA-WBRT, and thus lead to an enhanced memory preservation.(Gondi et al., 2014)

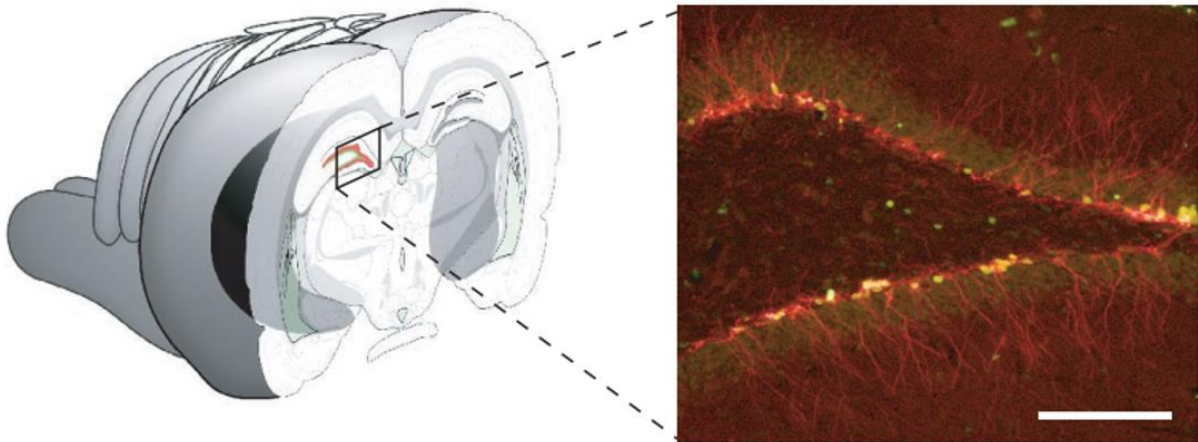


Figure 2. Schematic illustration of the anatomic location of the DG of the hippocampus within the rodent brain. DG was stained with the immature neuronal marker Dcx (red) and BrdU (green) was used to show proliferating cells (green).(Monje et al., 2003)

1.2 Pathophysiology of radiation-induced brain injury

Several proposed or prevailing pathophysiology mechanisms of radiation-induced CI in patients with metastatic or primary intracranial tumor have been elucidated. It is now clear that parenchymal and vascular cells are active participants in the response to radiation injury, and cellular response to radiation-induced brain injury relates to multiple cell types including astrocytes, microglia, oligodendrocytes,

endothelial cells, and neurons, which initiate neuroinflammatory cascades and contribute to progressive CI.(Moulder & Cohen, 2007; Tofilon & Fike, 2000) Preclinical and clinical studies support the hypothesis that a series of processes involving injury of neurovascular unit causing blood–brain barrier (BBB) disruption, NPC death, loss of hippocampal neurogenesis, and astrocyte senescence contribute to neuroinflammation.(Turnquist et al., 2020) (Figure 3)

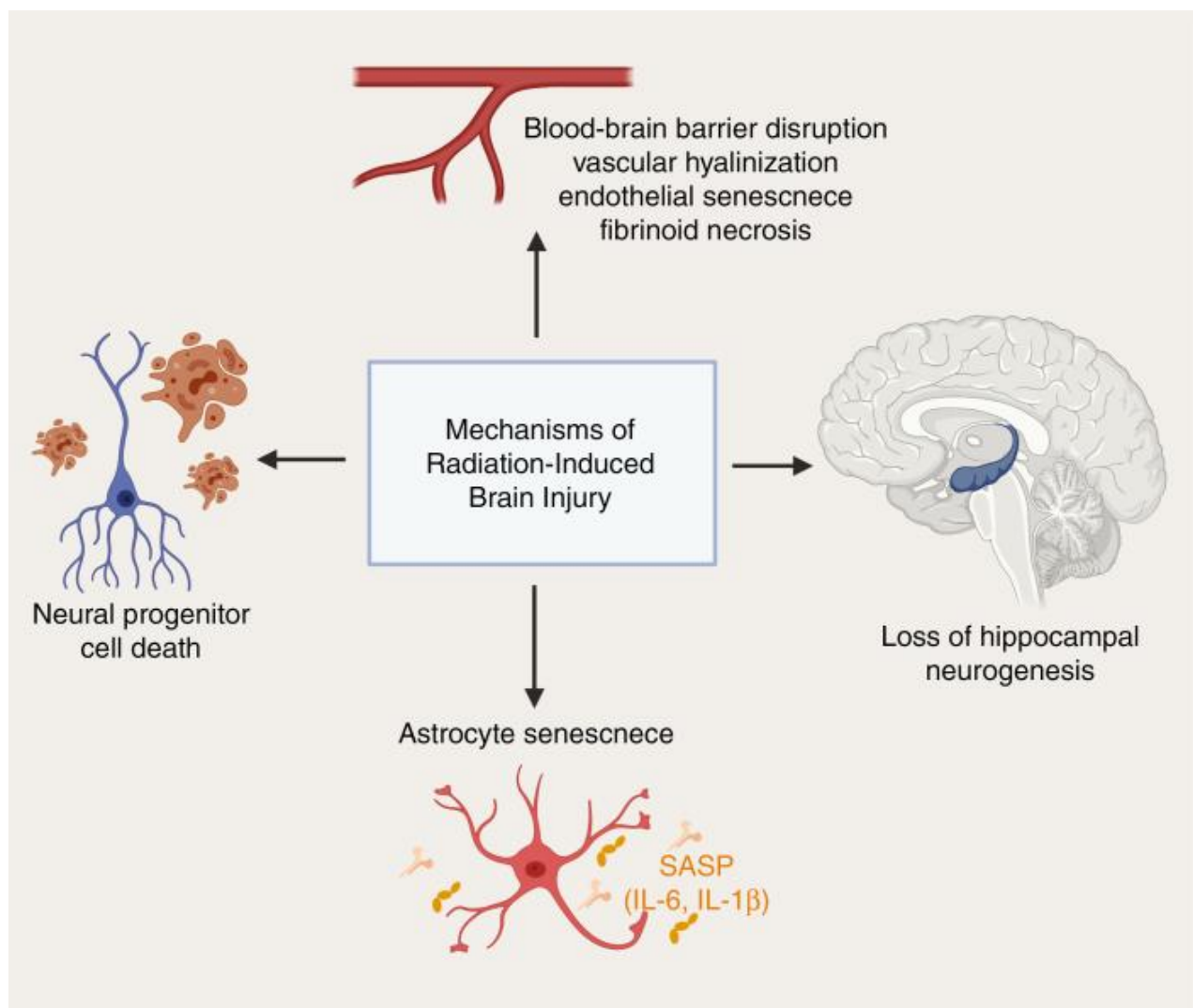


Figure 3. Pathophysiology mechanisms of radiation-induced brain injury. Vascular changes hypothesis including blood-brain barrier disruption, vascular hyalinization, endothelial senescence, and fibrinoid necrosis. Others include the loss of hippocampal neurogenesis, astrocyte senescence leading to senescence-associated secretory phenotype (SASP) cytokines, and NPC death.(Turnquist et al., 2020)

1.2.1 Radiation-induced vascular changes

Radiation not only affects vascular structural changes such as vessel wall thickening, vessel dilation, and induces endothelial cells death,(Calvo et al., 1988; Reinhold et al., 1990; Schultheiss & Stephens, 1992) but also reduce the number of endothelial cell nuclei, blood vessel density and length in a time and dose-dependent manner.(W. R. Brown et al., 2007; Reinhold et al., 1990) Additionally, capillary rarefaction and tissue hypoxia that is increased in the hippocampus after WBRT does not stimulate angiogenesis, and thereby leads to vascular damage and CI.(Warrington et al., 2011) Another vascular hypothesis is RT impact microvasculature result in ischemia and toxic neuroexcitation. Vascular changes following RT parallel vascular dementia, accelerated atherosclerosis and mineralizing microangiopathy in the microvasculature after RT eventually cause

vascular insufficiency and infarction (Danysz et al., 1998; Orrego & Villanueva, 1993), which could be one reason for ischemia. Therefore, the level of extracellular glutamate is increased. Serving as a potent activator of the postsynaptic NMDA receptors and the major excitatory neurotransmitter in CNS, increased glutamate triggers a considerable amount of calcium long lasting influx and subsequent activation of downstream signaling pathways. (Lai et al., 2014) It has been indicated that blocking excessive pathologic stimulation of NMDA receptors could protect patients of vascular dementia from further brain injury. (Lancelot & Beal, 1998; Orgogozo et al., 2002; Wilcock et al., 2002)

1.2.2 Blood brain barrier (BBB) disruption

Acute BBB disruption is well recognized after RT to the CNS since disruption BBB enable systemic immune and inflammatory cells to enter the brain and promote inflammation. The BBB consists of endothelial cells, pericytes, and astrocyte end-feet that form tight junctions, however, radiation leads to the destabilization of the plasma membrane of vascular endothelial cells. (Y. Q. Li et al., 2003) Moreover, endothelial cell apoptosis initiates acute BBB disruption and acute BBB disruption after radiation is mediated by the acid sphingomyelinase pathway in the

CNS.(Shinohara et al., 1997) It has also been reported that alterations in the BBB results in an imbalance in the levels of the matrix metalloproteinase-2 and the metalloproteinase-2 tissue inhibitor, and a degradation of collagen type IV, an extracellular matrix component of the blood vessel basement membrane.(T. C. Lee et al., 2012) In addition, a rapidly increased expression of vascular endothelial growth factor appears to play an important role in the radiation injury of the CNS, due to its impact on the BBB microvascular permeability.(Nordal et al., 2004)

1.2.3 Loss of hippocampal neurogenesis

The hippocampus is one of the regions of the animal brain that continues to produce neurons postnatally. An impairment of the hippocampal neurogenesis is a critical mechanism underlying CI. Neurogenesis occurs mainly in the hippocampal DG and subgranular zone (SGZ) and the subventricular zone (SVZ) of the lateral ventricles (LV).(Kuhn et al., 1996) Radiation-induced impairment of hippocampal neurogenesis and inhibition of NPC differentiation are associated with cognitive deficits in young and adult mice in the regions mentioned above.(Mizumatsu et al., 2003; Raber et al., 2004; Rola et al., 2004) An extreme sensitivity of adult neurogenesis to low doses of RT elucidated the negative effects of radiation on

cognitive dysfunction and the close relationship with hippocampal neurogenesis. Interestingly, although the initial response to radiation is similar in the SGZ and SVZ, the DG is severely affected long-term, whereas the SVZ appears to recover subsequently.(Gage, 2000; Hellstrom et al., 2009; Hellstrom et al., 2011) This differences in recovery could be attributed to growth factors, which were upregulated in SVZ microglia to increase the proliferation and decrease cell death of irradiated neuro-spheres in vitro.(Hellstrom et al., 2011)

1.2.4 NPC dysfunction

Neurogenesis deficit reflects alterations in the microenvironment that regulates progenitor cell fate, and a defect in the proliferative capacity of the NPC population. One prevailing hypotheses is that radiation induces neuro-inflammation and microvascular damage to the hippocampal SGZ and SVZ resulting in microenvironment changes in the NPC.(Monje et al., 2002) Age-related decrease of NPC proliferation persists in rats.(Kuhn et al., 1996) Furthermore, another study indicated that by intrahippocampal transplantation with human neural stem cells could provide a replacement for the loss of NPC, which functionally integrates into the hippocampus and ameliorates radiation-induced CI.(Acharya et al., 2011)

However, more detailed investigation are needed to determine the precise mechanism of radiation-induced NPC depletion.

1.2.5 Astrocyte senescence

Radiation induces not only apoptosis but also senescence which could be detected in brain, lung, and heart tissues.(Citrin et al., 2013; Wang et al., 2016) Accumulating evidence shows that cell senescence results in endothelial dysfunction by the induction of oxidative stress and inflammation as well as by an inhibition of angiogenesis.(Wang et al., 2016) Astrocytes protect the brain from oxidative damage(Wilson, 1997) and BBB dysfunction.(Janzer & Raff, 1987) SASP may contribute to the development of radiation-induced deleterious effects and respond to astrocytes after RT.(Turnquist et al., 2019) Besides, SASP is capable of transforming senescent fibroblasts to proinflammatory cells which could promote carcinogenesis.(Coppe et al., 2010) A recent study indicates that radiation-induced astrocyte senescence could be restored by Delta133p53, which is an inhibitory isoform of p53 that is characterized by promoting DNA double-strand break repair (DSB), and inhibition of astrocyte-mediated neuroinflammation and neurotoxicity.(Turnquist et al., 2019)

1.2.6 Dendritic morphological and functional change of mature neurons

Recent studies have focused on how radiation affects neuronal structure and function, due to the deficiency of the regeneration in the mature neurons. The CNS has a poor self-repair capability after radiation injury. Dendrites play a crucial role in neuronal function and signaling and dendritic morphology and physiological changes mirror the function of radiation-induced mature neurons.(Chakraborti et al., 2012; Hinkle et al., 2019; Kiffer et al., 2020; Raber et al., 2016; Shirai et al., 2013; Simmons et al., 2019; von Bohlen Und Halbach, 2009) A study has shown that radiation compromises neuronal architecture in the hippocampus which is reflected by a dose-dependent reduction in the number and density of dendritic spines.(Parihar & Limoli, 2013) (Figure 4) In case of neuronal function, electrophysiological recordings of ex vivo hippocampal brain slices demonstrated acute effects of radiation on neuronal cells in the DG region, including the inhibition of the long-term potentiation (LTP).(Wu et al., 2012) Since LTP represents a classical form of synaptic plasticity and provides the most promising neural correlate of learning and memory, it has been investigated in multiple preclinical and clinical

studies.(Cooke & Bliss, 2006) However, the detailed mechanism of radiation-induced dendritic alterations is still unknown.

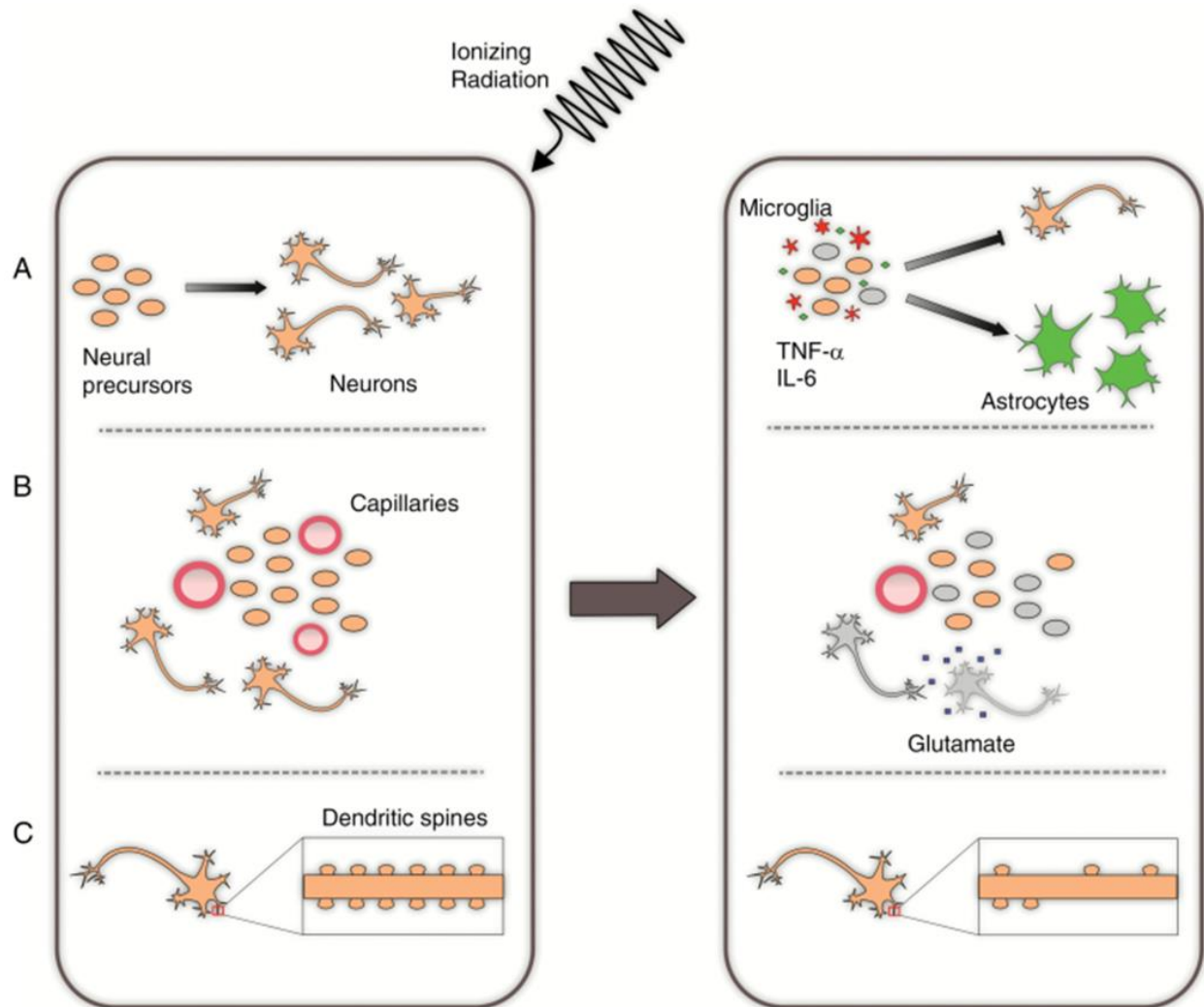


Figure 4. Schematic representation of radiation compromising dendritic spine density through excessive accumulation of glutamate in the hippocampus.(Parihar & Limoli, 2013)

1.3 Hippocampus

1.3.1 Introduction

The hippocampus is considered as one of the most thoroughly studied areas of the mammalian CNS, since it is characterized by its distinctive and identifiable macroscopic and microscopic (histological) structure and the hippocampus has long been considered as a key area for learning and memory since the 1950s.(Johnston & Amaral, 2004) Anatomically, the hippocampus consists of the DG, Cornu Ammonis 1 (CA1), CA2 and CA3 regions.(Michaelidesova et al., 2019)(Figure 5) The DG is the first relay station for the information processing, when information enters the hippocampus. Then it flows back from DG to CA3, then CA1 primarily receives excitatory input from CA3.(Witter et al., 2000) Although CA2 only occupies a small part of the hippocampus and usually its function is neglected, this small area seems to be resistant to massive cell destruction induced by epilepsy.(Hausler et al., 2016; Tulke et al., 2019) It is generally believed that each part of these regions plays a unique role in the processing of hippocampus information, but so far, the detailed functions of each area are not well understood. Most of the cellular mechanisms underlying memory formation reside in the long-term modulation of the synaptic efficacy, which is regulated by LTP and long-term

depression (LTD).(Massey & Bashir, 2007) While LTP represents synaptic strengthening and is important for the information storage, LTD is capable of shaping previously stored information and enhancing the information with respect to the signal-to-noise ratio.(Massey & Bashir, 2007) The interplay between these inhibitory and excitatory signaling underlie the synaptic plasticity.(Artola & Singer, 1993; Fagiolini & Hensch, 2000; Mulkey & Malenka, 1992)

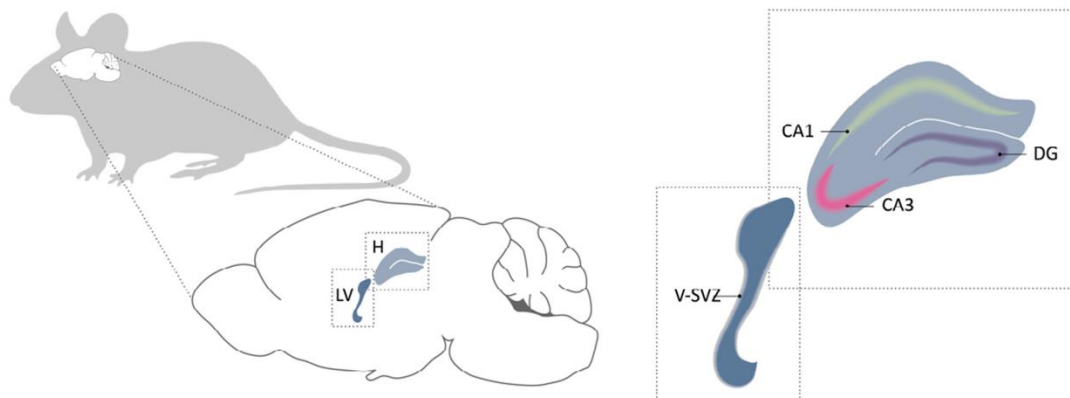


Figure 5. Sagittal view of the adult mouse brain focusing on two neurogenic niches where NSCs resides in the V-SVZ of the LV and DG of the hippocampus. CA1 and CA3 subfields of the hippocampus are shown.(Michaelidesova et al., 2019)

1.3.2 Role of hippocampus in radiation-induced CI

Although RT is widely applied in both adult and juvenile patients, radiation-induced cognitive deficits such as reduced verbal and spatial memory, attention and novel problem-solving ability, are particularly severe in the developing brain of young patients. Moreover, the incidence and severity of these cognitive deficits increase over time.(Roman & Sperduto, 1995) Neurocognitive impairment after WBRT is presumably mediated by radiation-induced damage of normal neuronal tissues. Preclinical juvenile animal models have shown that radiation-induced impairment of hippocampal neurogenesis is associated with cognitive deficits(Rola et al., 2004) which are similar to those observed in human hippocampal neurogenesis after brain RT.(Monje et al., 2007) Children are more vulnerable to RT than adults (Briere et al., 2008; Robison et al., 2009) and the intensity of cognitive symptoms correlate with the younger age of the child at the time of RT.(Chin & Maruyama, 1984; Duffner et al., 1985; F. P. Li et al., 1984; Packer et al., 1987) Presently, no effective treatment is available to ameliorate these deleterious radiation effects and the underlying mechanisms which are responsible for the impairment of cognitive functions after brain irradiation in children are not well understood.

Radiation-induced injury of the hippocampus is consistently associated with CI in patients who received WBRT.(Gondi et al., 2012; Gondi, Tome, et al., 2010; Redmond et al., 2013; Rola et al., 2004) High RT doses to the hippocampus of adults with primary brain tumors lead to an impairment in verbal fluency, executive function, and processing speed.(Haldbo-Classen et al., 2020) Moreover, a correlation of the radiation dose to the hippocampus and severe radiation-induced cognitive dysfunctions in children mainly ascribes to damaged NPCs residing in the hippocampus.(Redmond et al., 2013) Dynamic structural changes in hippocampal neurons of the DG are induced in mice receiving either 1 or 10Gy WBRT on day 30(Duman et al., 2018; Parihar & Limoli, 2013) and histopathological changes in the rat neurogenic region correlate with appropriate CI after a fractionated WBRT with 20Gy.(Balentova et al., 2018) Ex vivo studies on cultured, whole hippocampal slices demonstrated that functional neuronal deficiencies in the DG which are represented by an inhibition of LTP are induced by an irradiation dose of 10Gy.(Wu et al., 2012) A WBRT with 10Gy compromises neuroplasticity in both adult and juvenile rats on day 3 and induces age-dependent deficits along the hippocampal-prefrontal cortex pathway (PFC).(D. Zhang et al., 2018) Human synaptic LTP share molecular mechanisms with animal LTP(Cooke & Bliss, 2006) and deficits in LTP induction are associated with deficiencies in hippocampus-dependent memory in

humans. Therefore, measurements of LTP produced after high frequency stimulation (HFS) are considered as the most compelling cellular correlate of learning and memory.(Cooke & Bliss, 2006)

1.4 Aim of study

The vast majority of studies on LTP have been carried out in the CA1 region where LTP is particularly robust. Most of the excitatory input to CA1 pyramidal neurons originate from CA3 pyramidal cells located in both the ipsilateral and contralateral hippocampus.(Collingridge et al., 1983) Since to date no studies have investigated ipsilateral and contralateral hippocampus changes after a unilateral radiation, we comparatively assessed the physiological functions of LTP in the irradiated and non-irradiated juvenile hippocampus by LTP measurements.

It is known that WBRT induces dose-dependent apoptosis in endothelial cells(Y. Q. Li et al., 2003) and suppresses endothelial cell proliferation.(W. H. Lee et al., 2011)

Regarding these findings, we studied the effects of unilateral irradiation on the microvascular network of the hippocampus using the Efficient Tissue Clearing and Multi-Organ Volumetric Imaging (EMOVI) technique.(Hofmann et al., 2020) Combining EMOVI with multiplexed antibody-based immunolabeling enabled

quantification of the hippocampus vessel network in transparent brain tissues with conserved cellular morphology.

2. Materials and Methods

2.1 Materials

2.1.1 Equipment

Axopatch 200B Amplifier	Co. Molecular Devices (USA)
Bond Rx Staining Machine	Co. Leica (Germany)
Bridge Amplifier	Co. Npi electronic (Germany)
HC PL APO CS2 20x/0.75 IMM objective	Co. Leica Microsystems (Germany)
Leica TCS SP8 confocal microscope	Co. Leica (Germany)
Small-animal Radiation Research Platform	Co. Xstrahl (UK)
Vibrating microtome (HM 650 V)	Co. Microm International (Germany)

2.1.2 Software

Digidata 1200 interface	Co. Molecular Devices (USA)
Igor Pro 6.1	Co. WaveMetrics (USA)
ImageJ 2	National Institute of Health (USA)

Imaris version 9.5	Co. Bitplane AG (Switzerland)
Leica Application Suite X	Co. Leica Microsystems (Germany)
Lightning	Co. Leica Microsystems (Germany)
Muriplan	Co. Xstrahl (UK)
Pulse version 8.5	Co. HEKA Electronic (Germany)
SARRP control	Co. Xstrahl (UK)
WinLTP-program	Anderson and Collingridge

2.1.3 Consumables

μ-Slide 8 Well Glass Bottom	Co. ibidi (Germany)
Bepathen Eye and Nose Ointment	Co. Bayer Vital (Germany)
Bipolar tungsten electrodes (50 μm)	Co. Hugo Sachs Elektronik (Germany)
Borosilicate glass micropipettes	Co. Hugo Sachs Elektronik (Germany)
Cotton Applicator	Co. Nobamed Paul Danz (Germany)
Cover slips (8.5 x 8.5 mm)	Co. Thermo Scientific (USA)

Disposable Hypodermic Needle (Gr.20)	Co. B-Braun (Germany)
Double Edge Safety Razor Blades	Co. Wilkinson Sword (UK)
Histoacryl Tissue Adhesive	Co. B-Braun Surgical S.A. (Spain)
Scalpel (No.22)	Co. Feather (Japan)
Vasco Nitril Blue Glove (S)	Co. B-Braun (Germany)

2.1.4 Chemicals

D-(+)-Glucose	Co. Sigma-Aldrich (USA)
Dimethylsulfoxide	Co. Sigma-Aldrich (USA)
Eosin Y solution (0.5% aqueous)	Co. Sigma-Aldrich (USA)
Ethanol (≥99.8%)	Co. Sigma-Aldrich (USA)
Ethyl cinnamate	Co. Sigma-Aldrich (USA)
Fetal calf serum	Co. Thermo Scientific (USA)
Formaldehyde acid (≥37%)	Co. Carl Roth (Germany)
Hematoxylin	Co. Sigma-Aldrich (USA)

Hyaluronidase (Type IV-S)	Co. Sigma-Aldrich (USA)
Hydrogen Peroxide (30%)	Co. Sigma-Aldrich (USA)
IC Fixation Buffer	Co. Thermo Scientific (USA)
Isoflurane Isp-Vet	Co. Chanelle (Ireland)
Isopropanol	Co. Sigma-Aldrich (USA)
Magnesium chloride	Co. Sigma-Aldrich (USA)
Normal mouse serum	Co. Jackson Immunoresearch
Phosphate buffer saline (PBS)	Co. Sigma-Aldrich (USA)
Potassium chloride	Co. Sigma-Aldrich (USA)
Sodium bicarbonate	Co. Sigma-Aldrich (USA)
Sodium chloride	Co. Sigma-Aldrich (USA)
Sodium phosphate monobasic	Co. Sigma-Aldrich (USA)
Triton X-100	Co. Carl Roth (Germany)
Type F Immersion liquid (RI = 1.518)	Co. Leica Microsystems (Germany)

2.1.5 Antibodies

Anti-CD31 (PECAM-1) antibody

Co. BioLegend (USA)

Phospho-Histone H2A.X rabbit mAb (9718)

Co. Cell Signaling Technology (USA)

2.1.6 Buffers and solutions

Artificial Cerebrospinal Fluid (aCSF) Solution

7.305g	125 mmol/L	NaCl
0.186g	2.5 mmol/L	KCl
0.172g	1.25 mmol/L	NaH ₂ PO ₄ -Monohydrate
4.954g	25 mmol/L	D-(+)-Glucose-Monohydrate
2.100g	25 mmol/L	NaHCO ₃
0.203g	1 mmol/L	MgCl ₂ -Hexahydrate
0.294g	2 mmol/L	CaCl ₂ -Dihydrate
1000ml		dH ₂ O

2.2 Methods

2.2.1 Animal care and partial-brain radiation (PBRT) procedure

All in vivo animal experiments were performed in full compliance with the institutional guidelines of the Technical University of Munich and with approval from the Government District of Upper Bavaria (protocols number 55.2-1-55-2532-75-2015). All health checks and hygiene measures were performed according to FELASA guidelines.(Guillen, 2012) All efforts were made to minimize animal suffering and to reduce the number of animals.

Female 5-week-old juvenile C57BL/6 mice (Charles River, USA) were used in all experiments. Animals were housed with food and water ad libitum in a temperature-controlled room ($23\pm 0.5^{\circ}\text{C}$) with a 12-hour light/dark cycle. Image-guided partial irradiation was performed on mice using a small-animal radiation research platform (SARRP, Xstrahl, UK). (Figure 6) On day 0, mice were anaesthetized by isoflurane/oxygen inhalation for the duration of the procedure. Transverse, sagittal and frontal computed tomography scans using 60 kV and 0.8 mA photons were performed for each mouse for precise radiation targeting.(Estrada et al., 2020; Sievert et al., 2018) The irradiation targeted 40% of the left brain volume with a beam size of approximately $(6\times 8)\text{ mm}^2$ and with a mean

target dose of 2, 4, 8, or 20Gy using 220 kV and a 13 mA X-ray beam filtered with copper (0.15 mm). For the fractionated dose group, mice were irradiated to a dose of 4Gy for two consecutive days. SARRP control and Muriplan software (both Xstrahl, UK) were used for CT imaging, precise radiation targeting, and calculating the irradiation dose. Five mice received partial brain irradiation and five were sham radiated. All mice fully recovered after the procedure and were housed in single ventilated cages under pathogen-free conditions until in vitro electrophysiology recording.

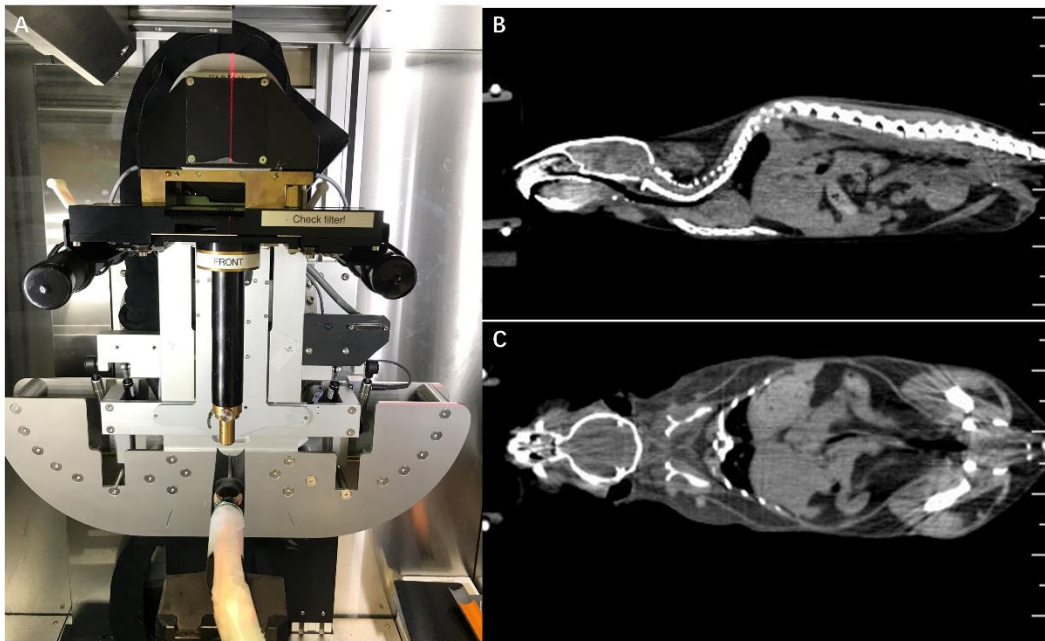


Figure 6. (A) Picture of the SARRP used in this study. (B) and (C) CT scan for mouse body.

2.2.2 Randomization and blinding

Mice were randomly assigned to experimental groups by a third party not involved in the study; group allocation was revealed only after complete analysis of the data. Radiation, preparation, and evaluation of histological specimens as well as (statistical) analysis of results were performed in a single blinded fashion.

2.2.3 Protocol for the assessment of the effect of PBRT on juvenile murine unilateral hippocampal synaptic plasticity and microvascular

Experimental groups included sham, 2Gy, 4+4Gy, 8Gy, and 20Gy mice (n=5/group). treated with PBRT. Body weight was measured on the day of PBRT, and at 5 weeks, 10 weeks after radiation. γ H2A-X staining was performed 1 hour after PBRT with 20Gy. Electrophysiological assays were performed 3 days, 5 weeks and 10 weeks after PBRT. Microvascular analysis was performed on hippocampi harvested 5 and 10 weeks after irradiated with 8Gy or 20Gy. (Figure 7)

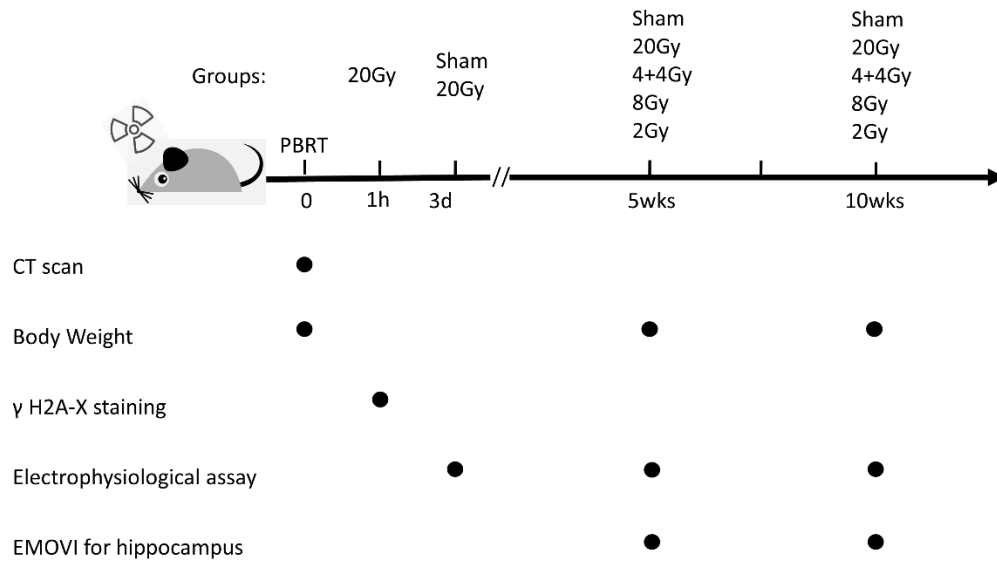


Figure 7. Schematic of PBRT mice project design.

2.2.4 Immunohistochemistry (IHC)

The precise delivery of the irradiation beam was confirmed using the DNA damage repair marker γ H2A-X on a Bond Rx staining machine (Leica) using a Polymer Refine detection system without post primary reagent. Due to γ H2A-X can be produced within a few minutes after DSBs induced by ionizing radiation, then reaches the peak in 30 minutes, and subsequently decreases over time. (Hunt et al., 2013) Therefore, brain was removed 1 hour after irradiation with 20Gy. Tissue was fixed in formalin overnight and embedded in paraffin. Blocks were sectioned in 2-

mm slices and stained with eosin (eosin γ -solution 0.5% w/v aqueous) and hematoxylin to visualize tissue structure, according to standard protocols.

2.2.5 Electrophysiological field recording

On days 3, 35 and 70 after irradiation, mice were deeply anaesthetized with isoflurane and decapitated. The brain was rapidly removed and placed into ice-cold aCSF solution containing 125 mM NaCl, 2.5 mM KCl, 25 mM NaHCO₃, 2 mM CaCl₂, 1 mM MgCl₂, 25 mM D-glucose, and 1.25 mM NaH₂PO₄, bubbled with a 95% v/v O₂, 5% v/v CO₂ mixture, and had a final pH of 7.3, saturated with carbogen gas (95% v/v O₂, 5% v/v CO₂; later referred to as carbogen). Sagittal slices (350 μ m thick) from left irradiated hemisphere and right non-irradiated hemisphere were prepared using a microtome (HM 650 V; Microm International, Walldorf, Germany) at 4°C. Both left and right slices were allowed to firstly recover for 30 min at 34°C and afterwards for at least 1h at room temperature in two submerged chambers containing aCSF and constantly aerated with carbogen. Afterwards the slices were transferred into the recording chamber for extracellular recordings. The flow rate of the solution through the chamber was 5 ml/min under continuous application of 0.3-0.5 l/min carbogen. The experiments were performed at room temperature.

Extracellular recordings of field excitatory postsynaptic potentials (fEPSPs) were evoked by stimulation of the Schaffer collateral commissural pathway in the dendritic region of hippocampal CA1 region and obtained using borosilicate glass micropipettes (1–2M Ω) (Hugo Sachs Elektronik-Harvard Apparatus, March-Hugstetten, Germany) filled with aCSF. fEPSP were evoked by alternately delivering a test stimulus (20 μ s, 4-5 V) via one of two bipolar tungsten electrodes (Hugo Sachs Elektronik-Harvard Apparatus, insulated to the tip; 50 μ m tip diameter), placed at either side of the recording pipette, thus stimulating non-overlapping populations of the Schaffer collateral commissural pathway. Stimulus frequency was 0.033 Hz per electrode. For baseline recordings, stimulation intensity was adjusted to values evoking a response of approximately 25-30% of the maximum response. Stable baseline recordings were made for at least 20 minutes before application of tetanic stimuli. LTP was then induced by delivering a HFS train (100 pulses delivered at 100 Hz) via one of the stimulating electrodes. We used both stimulating electrodes to utilize the input specificity of LTP and thereby allow the measurement of an internal control monitoring the vitality and hence the stability of neuronal activity of the slice. Thereafter, recordings were continued for an additional 60 min at the stimulation settings used for baseline recordings. Data were amplified (Axopatch 200B amplifier, Axon Instruments, Foster City, CA, USA or BA-2S, npi electronic,

Tamm, Germany, respectively), filtered (3 kHz) and digitized (Digidata 1200 interface, Axon Instruments, software WinLTP-program, <http://www.winltp.com/Ltp24/indexLtp24.htm> (Anderson and Collingridge, 2001) or Pulse version 8.5, HEKA Electronic GmbH, Lambrecht, Germany, respectively). Two consecutive signals of the respective input were averaged for analysis, resulting in one data point per minute. Offline data analysis was performed with Igor Pro v6.1 (Wavemetrics Lake Oswego, OR, USA). The fEPSP slope was measured between 20% and 80% of peak amplitude and presented as % EPSP slope of baseline.

2.2.6 Hippocampi staining and clearing using EMOVI

2.2.6.1 EMOVI sample preparation

Hippocampi (Figure 8B) were harvested from sacrificed mice after receiving 8Gy, 20Gy, 5 and 10 weeks, after irradiation, then fixed in IC Fixation Buffer (eBioscience) for 1 h at room temperature (RT) and in 25% (v/v) fixation buffer in PBS overnight at 4 °C. All following incubations were performed in 2 mL tubes or flat bottom plates with gentle agitation.

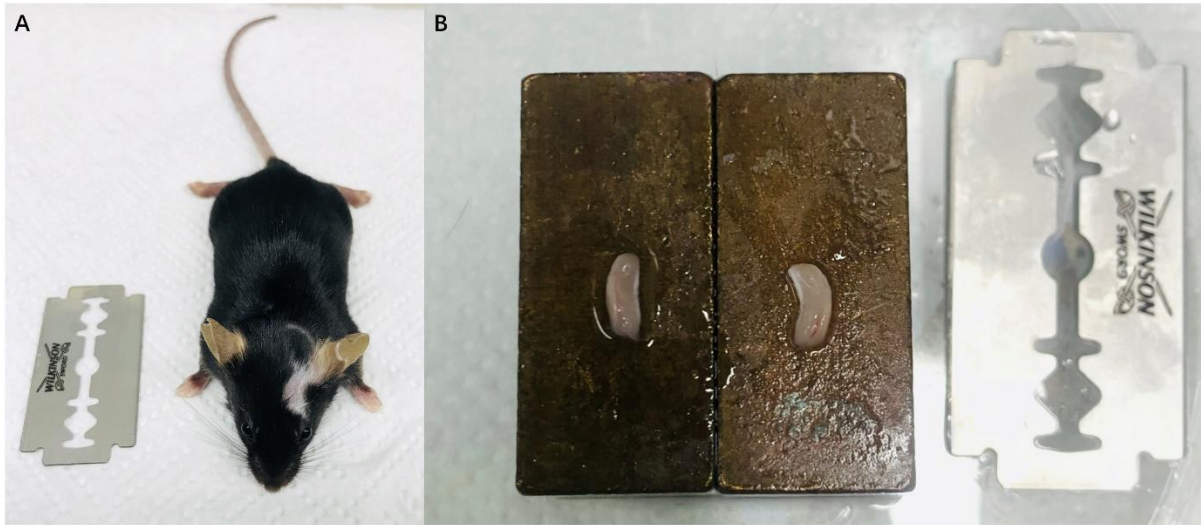


Figure 8. (A) Anesthetized mice treated with PRRT 20Gy after 10 weeks. (B) Left and right intact hippocampi were removed with a razor blade from the intact mouse brain.

2.2.6.2 Digestion

Samples were washed in PBS with 1% (v/v) FCS, 1% (v/v) normal mouse serum (Jackson ImmunoResearch) and 0.3% (v/v) Triton X 100 ('Blocking Buffer') for 1 h at 37 °C and incubated with 300 µg/mL hyaluronidase (from bovine testes, Type IV-S; Sigma Aldrich) in PBS for 2 h at 37 °C. After digestion, tissues were washed again for 1 h to remove remaining enzyme.

2.2.6.3 Antibody staining

Tissues were incubated in Blocking Buffer overnight for at least 12 h at 37 °C and stained with directly fluorochrome-conjugated, primary antibodies, diluted 1:100 in Blocking Buffer, for 72 to 96 h at 37 °C. The following steps were performed in the dark.

2.2.6.4 Dehydration and clearing

Stained samples were washed in PBS with 0.2% (v/v) Triton X 100 and 0.5% (v/v) 1-thioglycerol for 16 hours at 37 °C. Tissues were then dehydrated with ascending dilutions of 30, 50, 70, 100 and 100% (v/v) isopropanol (pH ~9) for 1 h each. Samples were then bleached with an at least one week old solution of 5% (v/v) hydrogen peroxide and 5% (v/v) DMSO in isopropanol for 4 h at 4 °C and again fully dehydrated in 100% (v/v) isopropanol for 1 h at 4 °C. To avoid ethyl cinnamate (ECi)-mediated freezing damage the samples were allowed to warm up to RT before samples were submerged in undiluted ECi for refractive index matching was applied. As ECi can dissolve a variety of polymers and samples could only be cleared and stored in Eppendorf 2 mL tubes.

2.2.6.5 Image acquisition

Cleared samples were mounted on glass coverslip bottom slides (ibidi) submerged in ECI and weighed down with an additional coverslip to limit movement during imaging. After image acquisitions, sample and clearing agent were removed from the chamber to conserve the slides for a later reuse.

Imaging was performed on an inverted Leica TCS SP8 confocal microscope with White Light Laser and HyD photodetectors using a HC PL APO CS2 20x/0.75 IMM objective (zoom factor of 1). The following acquisition settings were applied: 2048x2048 logistical size, 400 Hz scan speed, bidirectional scan mode, 4x line average, system optimized z-step size, sequential scans between frames, active time gating and 0.7 A.U. pinhole.

2.2.6.6 Data processing and analysis

Further data processing was performed on a Z640 Workstation (HP; Win10 Enterprise 64-bit; Intel Xeon CPU E5-2650 v3 @ 2.30GHz; 32.0 GB RAM; NVIDIA Quadro K2200 4 GB GDDR5 (DirectX 12.0)).

Contrast adjustment for display purposes and image analysis was performed using Imaris (Bitplane) version 9.5. We used the 'Surface Creation Wizard' in Imaris (Bitplane) to translate fluorescence data of CD31-labelled vessels into volumetric, representative surfaces, which we used for binary masking of the vessel structure. We next applied the 'Filament Creation Wizard' for looped structures in Imaris (Bitplane) onto the binarized fluorescence signal to automatically trace the vessel path as quantifiable filament objects.

All relevant statistics of objects were then exported as a collection of csv files and subsequently edited and concatenated into a single summary file using a recently published open-access Python application (https://gitlab.com/kepplerlab/imaris_statistics_converter).

2.2.7 Statistical analysis

Data for all groups were compared using a one-way ANOVA with Turkey's multiple comparisons test in GraphPad Prism. All results are shown as (mean \pm SEM). All statistical comparisons for the vascular parameters were made pair wise using the Student's t-test. Statistically significant differences of $p < 0.05$ are indicated by an asterisk (*) in the figures.

3. Results

3.1 PBRT of the left hemisphere of mouse brains

The left hemisphere of all mouse brains was irradiated using the SARRP with 3 lateral beams (5x5, 3x3, and 3x3 mm²) without any radiation overlap. This covers a total radiation field of approximately 6x8 mm² (Fig. 9A-C). To avoid radiation-induced damage in the cerebellum and optical nerves, only approximately 40% of the total brain volume received a mean target dose of 20Gy, as shown in the dose-fractionated volume curve (Fig. 9D). The dose distribution in the brain tissue, as visualized by IHC staining using the DNA DSB-repair marker γ -H2A.X (Fig. 9E), demonstrated precise targeting of the beam to the left hippocampus (LH 20Gy, Fig. 9F) which spared more than 90% of the right hippocampus (RH 0Gy, Fig. 9G).

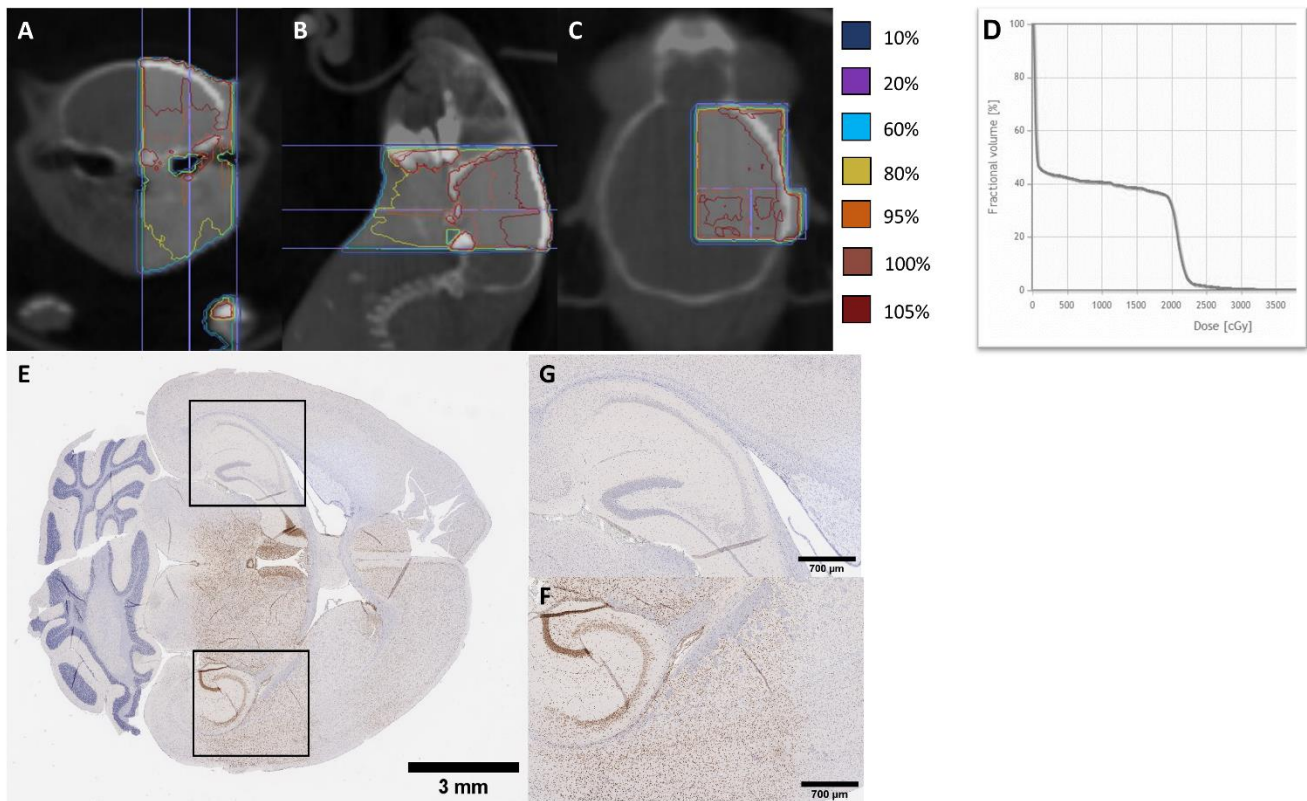


Figure 9. Irradiation protocol and γ -H2A.X-stained section CT scans acquired on the SARRP device in the coronal (A), sagittal (B) and axial (C) planes. Panel (D) shows Dose-Fractional Volume showing that approximately 40% of the left hemisphere absorb 20Gy. γ -H2A.X-stained section from a mouse brain that received 20Gy through a 5×5 mm square beam, and two 3×3 mm square beams (E). Right non-irradiated hippocampus (G) and the intended target was the left irradiated hippocampus (F).

3.2 PBRT inhibits LTP in the CA1 region of hippocampal slices 3 days after radiation

Next, the effects of PBRT (20Gy) on CA1-LTP were determined on day 3 (Fig. 10a). No significant differences ($P>0.999$) were observed in the sham groups (LH Sham, RH Sham) after conditioning stimuli. The fEPSP slope of left and right hippocampal slices (LH/RH) were $136.5\pm 1.6\%$ and $136.9\pm 2.6\%$ ($n=5$), respectively (Fig. 10b). On day 3 after irradiation (20Gy) of the left hemisphere of juvenile mice, LTP in the left irradiated hippocampal (LH 20Gy) slices was severely impaired and synaptic responses decreased significantly to $106.5\pm 1.0\%$ ($n=5$) compared to that of the sham (LH Sham) and the non-irradiated right hippocampus (RH 0Gy) group (LH 20Gy vs. LH Sham, $P=0.0079$; LH 20Gy vs. RH 0Gy, $P=0.0093$). These findings are in line with results of previous studies analyzing acute effects of radiation on neuronal cells in isolated brain slices in vitro receiving a single dose of 10Gy. (Wu et al., 2012) The analysis of the difference in LTP values in the four groups, as determined by ANOVA, revealed significant differences ($F_{(3,16)}=7.143$, $P=0.0029$). Interestingly, in contrast to the radiation-induced LTP inhibition in the irradiated left hippocampus (LH 20Gy), no significant differences were observed between non-irradiated right hippocampal slices and that of the sham group (RH 0Gy vs. LH Sham, $P=0.9998$; RH 0Gy vs. RH Sham, $P=0.9991$).

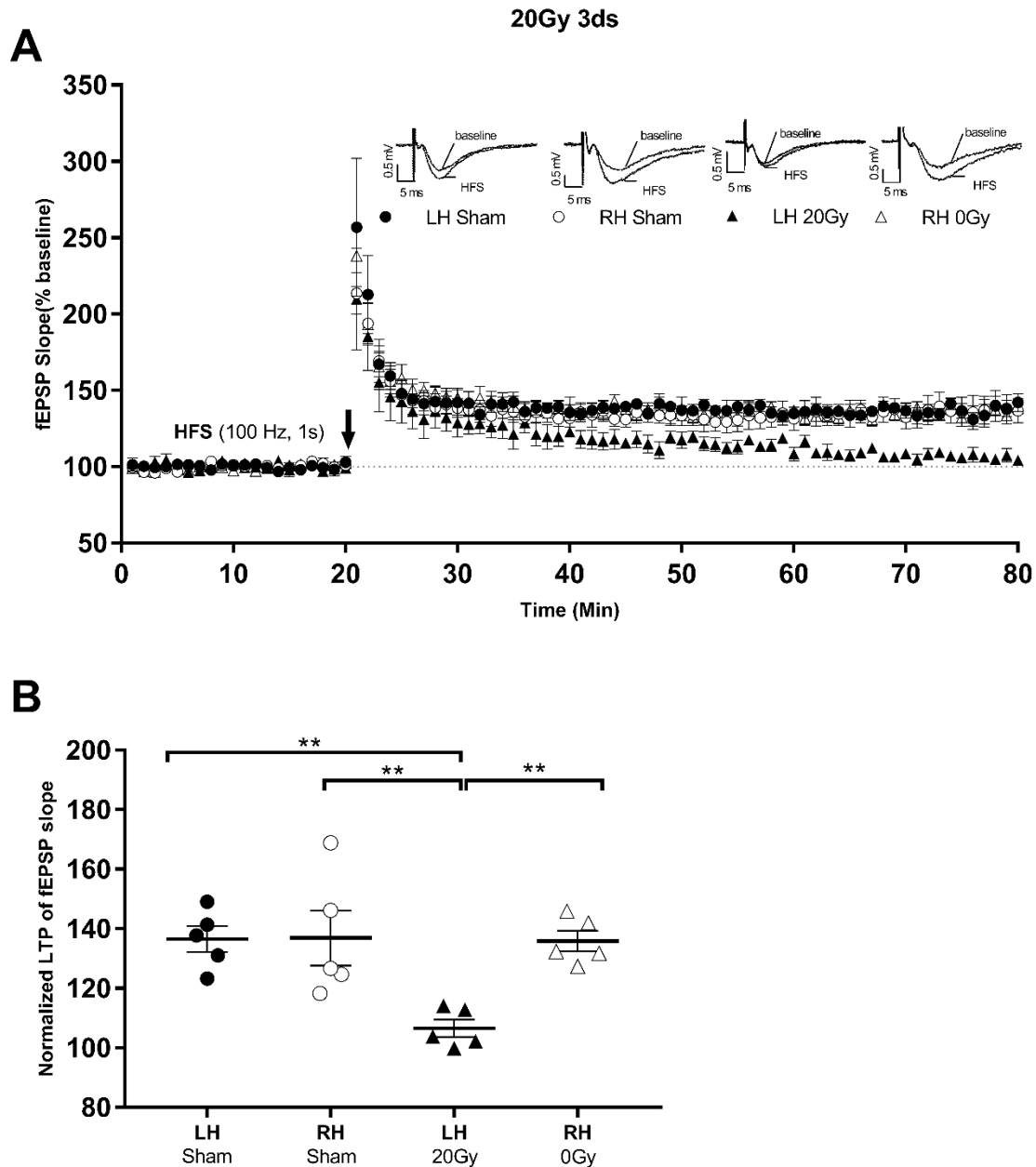


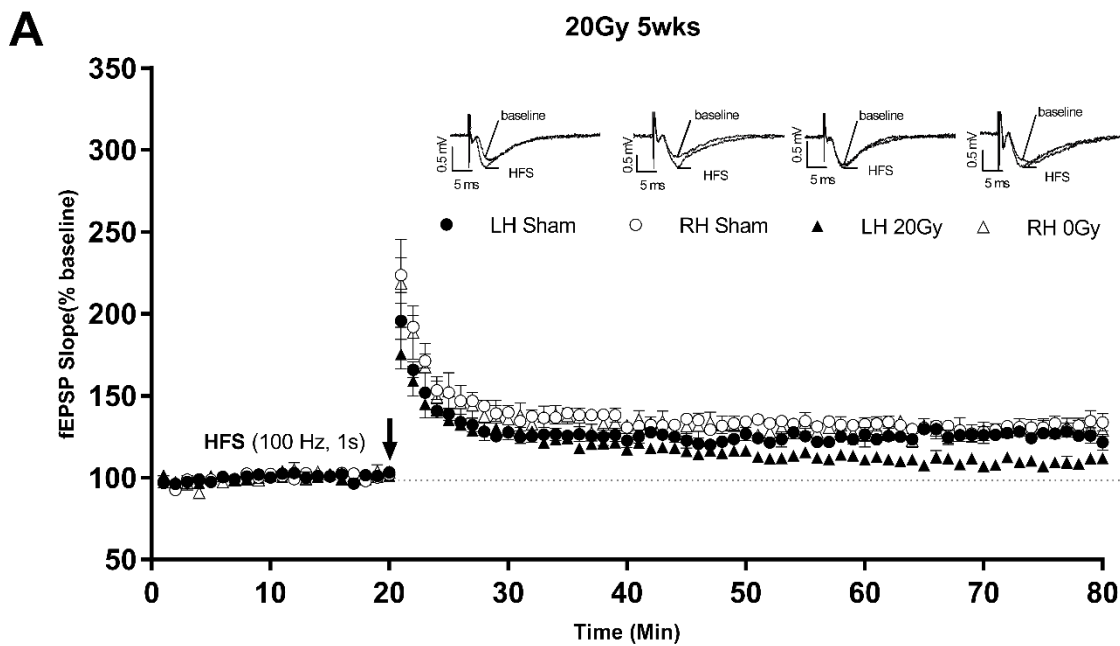
Figure 10. PBRT inhibits CA1-LTP of irradiated hippocampal slices. (A) The panel A shows the time course for the induction/maintenance of LTP following tetanic stimulation of the Schaffer collateral to CA1 pathway both in murine irradiated and non-irradiated hippocampal slices at day 3 after 20Gy irradiation. fEPSP slopes

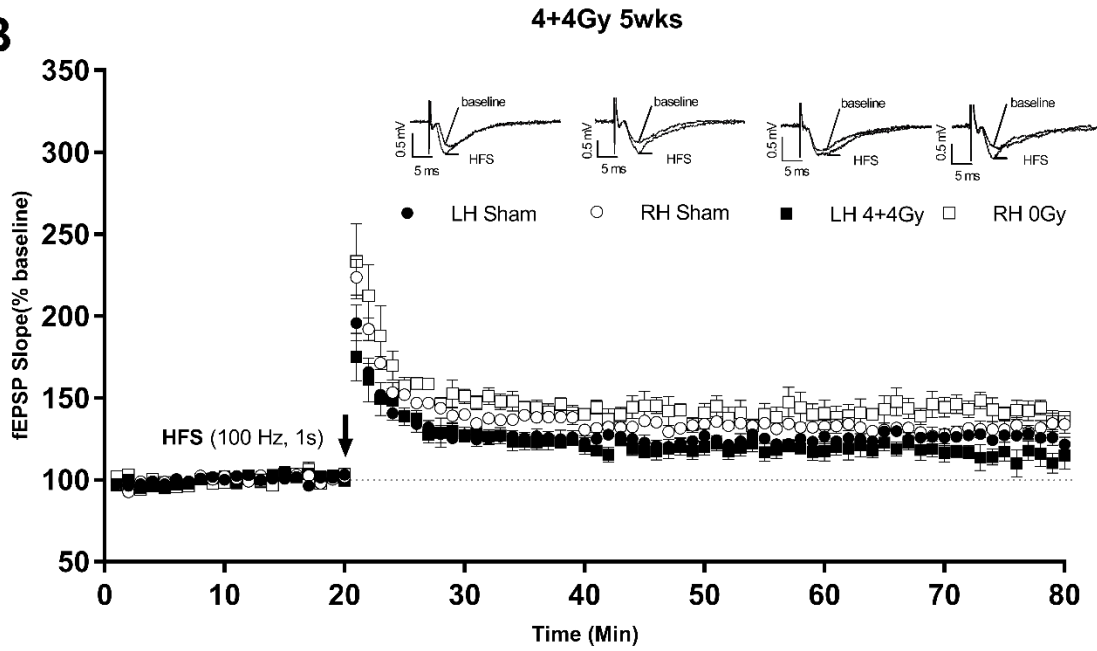
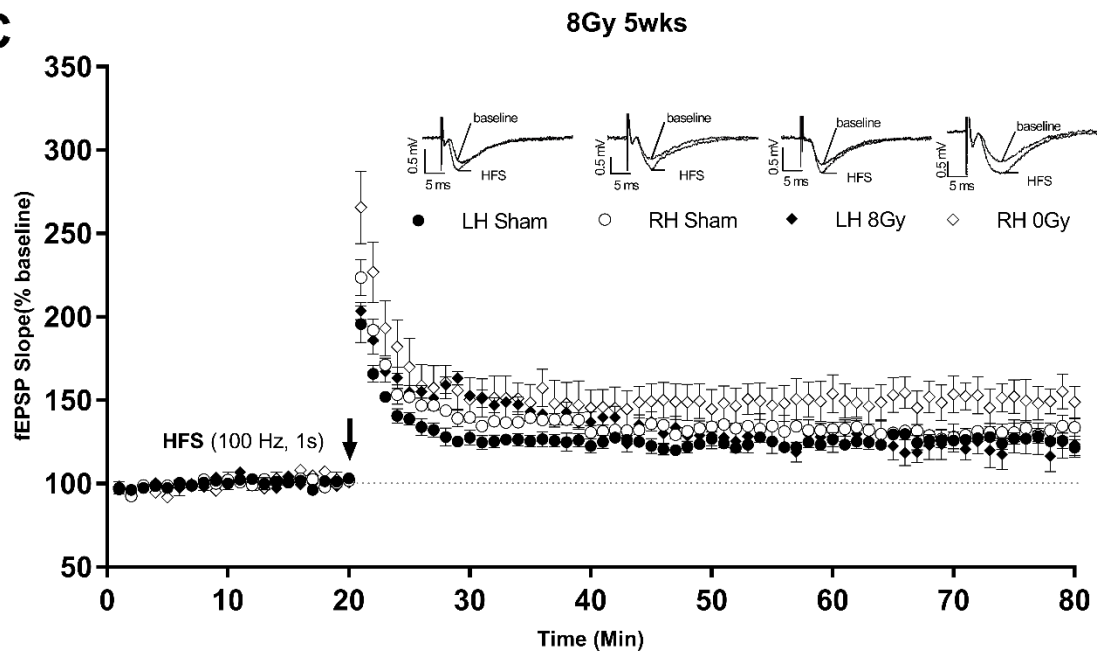
(means±standard error of the mean, SEM) are blotted against time and responses were normalized to baseline levels recorded 20 min prior to delivering HFS (arrow). Insets show representative fEPSP traces before and after HFS. In contrast to the left (dark grey circles, n=5) and right (open circles, n=5) hippocampal slices of sham mice, PBRT given at a single dose of 20Gy markedly inhibits LTP 3 days after irradiation in the ipsilateral (dark grey triangles, n=5) but not contralateral (open triangles, n=5) slices. (B) Respective scatter plot summarizing the last 50 to 60mins after HFS. One-way ANOVA with repeated measures showed significant differences between sham and irradiation groups [$F_{(3,16)}=7.143$, $P=0.0029$]. ** $P < 0.01$ vs. sham groups.

3.3 LTP in irradiated hippocampal slices was blocked by different PBRT regimen, while unaffected in the contralateral hippocampus

In a next set of experiments we applied a PBRT in juvenile mice (n=5 per group) with clinically relevant single doses of 2, 8, a fractionated dose of 4+4Gy and 20Gy. Identical stimuli were applied to induce LTP, 5 weeks after radiation (Fig. 11A-D). LTP signals significantly decreased after 5 weeks in the irradiated LH 20Gy group (109.7%±0.7%) [$F_{(3,16)}=9.78$, $P=0.0007$ vs. Sham] and 4+4Gy group (114.7%±1.8%)

[$F_{(3,16)}=7.15$, $P=0.0029$ vs. Sham] (Figure 11E), whereas no significant differences were observed in the LH 2Gy [$F_{(3,16)}=1.88$, $P=0.1732$] and LH 8Gy groups [$F_{(3,16)}=3.22$, $P=0.0504$]. Moreover, the HFS-induced potentiation of fEPSPs in the non-irradiated right hippocampus (RH) of juvenile mice remained normal, and no changes in the fEPSP slope were detected 5 weeks after PBRT. LTP in slices of the non-irradiated RH 0Gy remained unchanged even though the corresponding left hemispheres received 20Gy (Fig. 11E).



B**C**

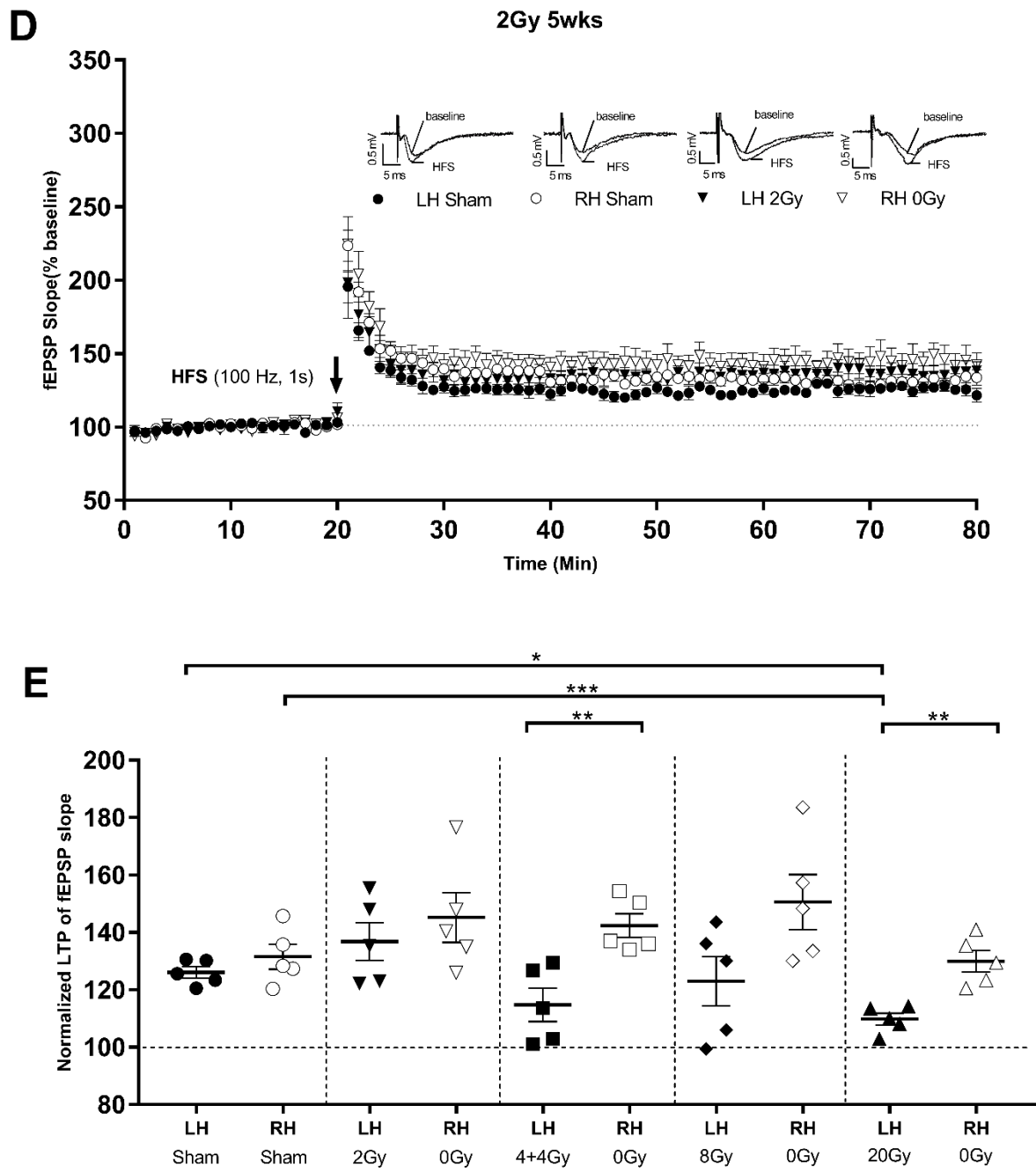
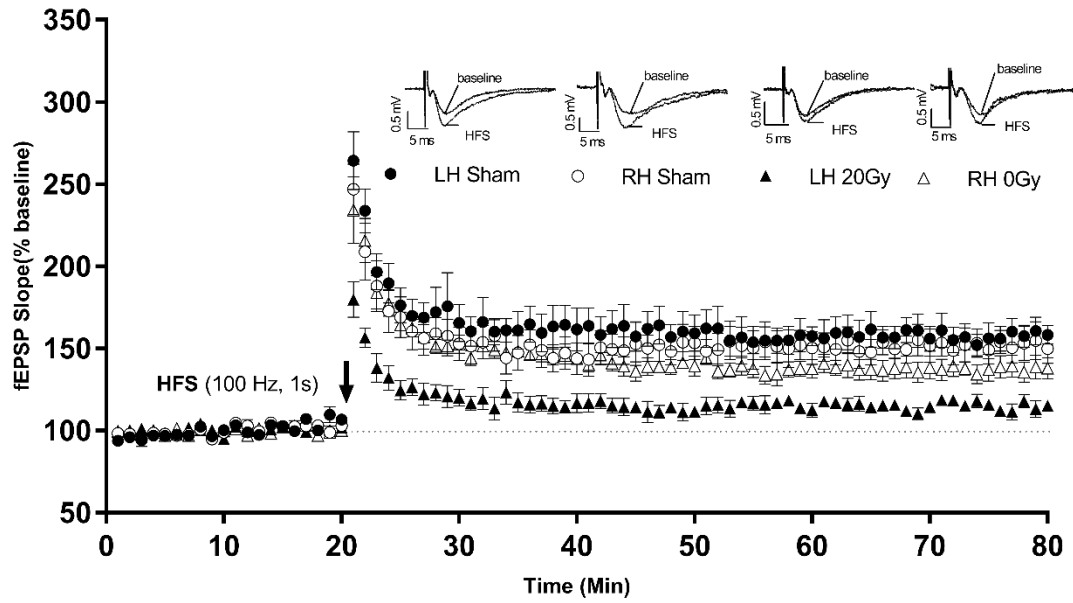
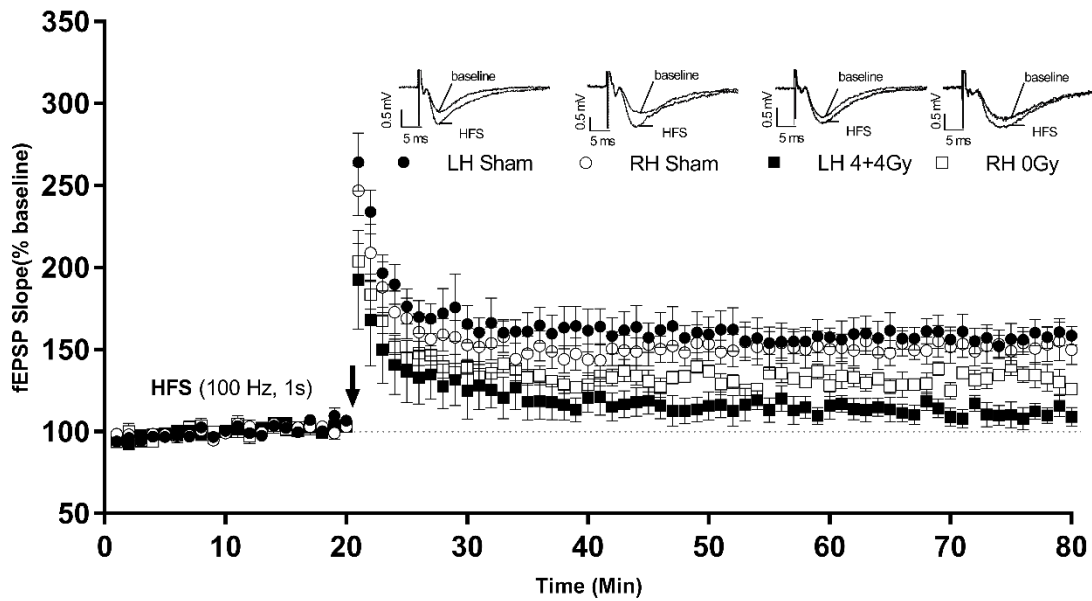


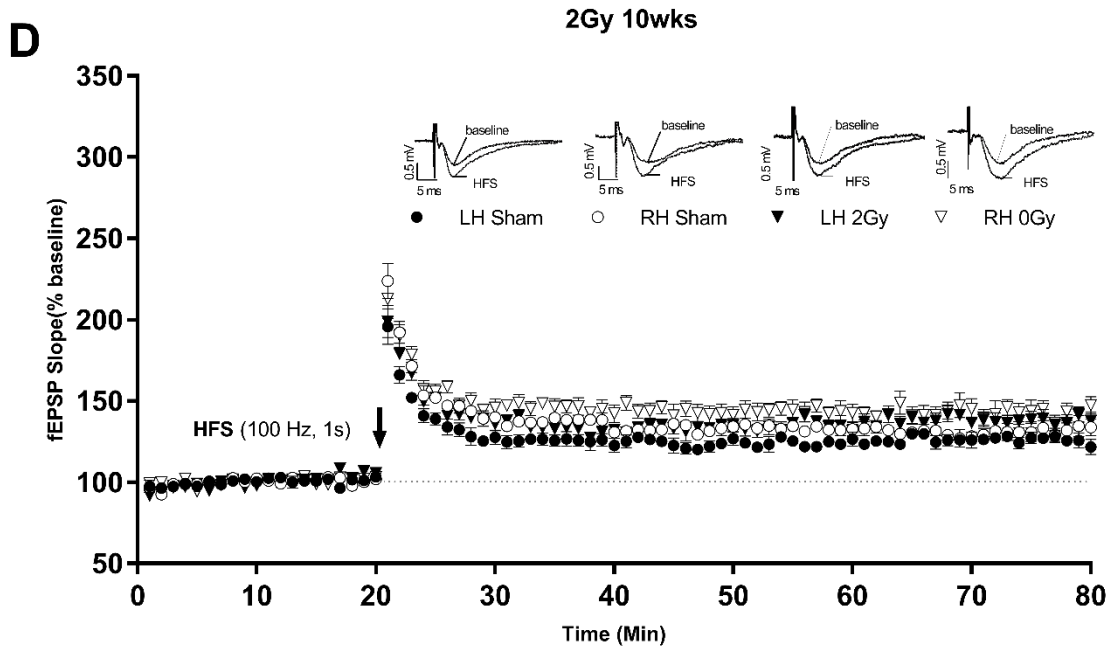
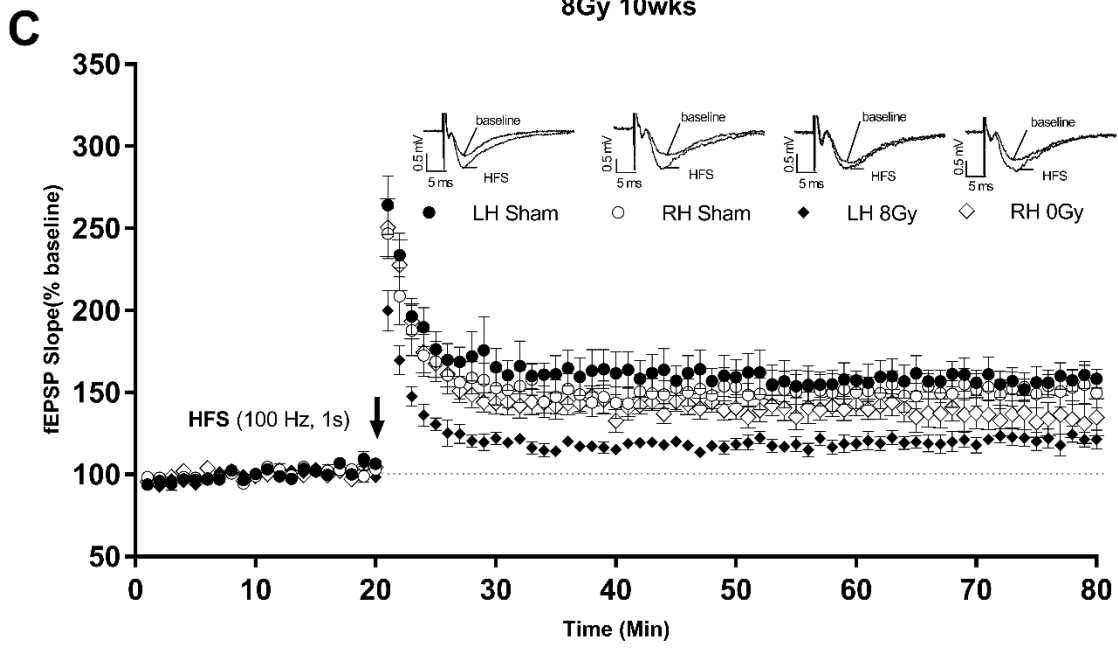
Figure 11. After 5 weeks recovery from PBRT, LTP in hippocampal slices is inhibited dose-dependently. CA1-LTP was measured in left/right hippocampal

slices of sham group and irradiated/non-irradiated slices of radiation group 5 weeks after (A) single dose of 20Gy, (B) fractionated dose of 4+4Gy, (C) single dose of 8Gy and (D) single dose of 2Gy. (E) Scatter plot of averaged values 50-60mins post HFS delivery. Postsynaptic potentials in juvenile mouse left/irradiated and right/non-irradiated hippocampal slices were $126.0\% \pm 1.0\%$ (averaged LTP values of 5 independent samples) and $131.5\% \pm 1.4\%$ of sham groups, $136.7\% \pm 1.9\%$ and $145.1\% \pm 2.6\%$ after 2Gy, $114.7\% \pm 1.8\%$ and $142.3\% \pm 1.6\%$ after 4+4Gy, $123.0\% \pm 2.6\%$ and $150.5\% \pm 2.8\%$ after 8Gy, $109.7\% \pm 0.7\%$ and $129.9\% \pm 1.2\%$ after 20Gy (5 mice per group), respectively. Analysis of LTP in sham and 4+4Gy groups [$F_{(3,16)}=7.15$, $P=0.0029$], 20Gy groups [$F_{(3,16)}=9.78$, $P=0.0007$] revealed significant differences, however, no significant differences in neither 2Gy groups [$F_{(3,16)}=1.88$, $P=0.1732$] nor 8Gy groups [$F_{(3,16)}=3.22$, $P=0.0504$] were detected. LTP in LH of 20Gy (Left hippocampus of 20Gy) was still significantly blocked ($109.7\% \pm 0.7\%$, $P<0.05$ vs. LH Sham; $P<0.001$ vs. RH Sham). LTP in non-irradiated hippocampal slices remained stable throughout the different dose regimen: 2Gy groups ($145.1\% \pm 2.6\%$, $P=0.1449$ vs. LH Sham; $P=0.3907$ vs. RH Sham), 4+4Gy groups ($142.3\% \pm 1.6\%$, $P=0.0700$ vs. LH Sham; $P=0.3147$ vs. RH Sham), 8Gy groups ($150.5\% \pm 2.8\%$, $P=0.0949$ vs. LH Sham; $P=0.2439$ vs. RH Sham) and 20Gy groups ($129.9\% \pm 1.2\%$, $P=0.8259$ vs. LH Sham; $P=0.9849$ vs. RH Sham) were detected during this period. * $P<0.05$ vs. sham groups.

3.4 LTP in juvenile mice remained inhibited at 10 weeks after irradiation

To further explore long-term effects in the irradiated (LH) and non-irradiated (RH) hippocampus, juvenile mice ($n=5$) were irradiated with the same radiation regimen as shown before and evaluated after 10 weeks. Significant reductions in LTP were observed between sham and LH 4+4Gy [$F_{(3,16)}=9.32$, $P=0.0008$], sham and LH 8Gy [$F_{(3,16)}=4.12$, $P=0.0241$] and sham and LH 20Gy irradiated groups [$F_{(3,16)}=7.78$, $P=0.002$] (Figure 12A-D). No changes in the fEPSP slopes were observed in the non-irradiated right hippocampus (RH) groups after irradiation of the LH with 2Gy ($P=0.8318$ vs. LH Sham; $P=0.9901$ vs. RH Sham), 4+4Gy ($P=0.0990$ vs. LH Sham; $P=0.2549$ vs. RH Sham), 8Gy ($P=0.2256$ vs. LH Sham; $P=0.4458$ vs. RH Sham) and 20Gy ($P=0.1971$ vs. LH Sham; $P=0.4525$ vs. RH Sham). Although RH LTP values in the 4+4Gy and 20Gy groups were slightly lower than those of the sham group, they did not differ significantly and were within the normal range.

A**20Gy 10wks****B****4+4Gy 10wks**



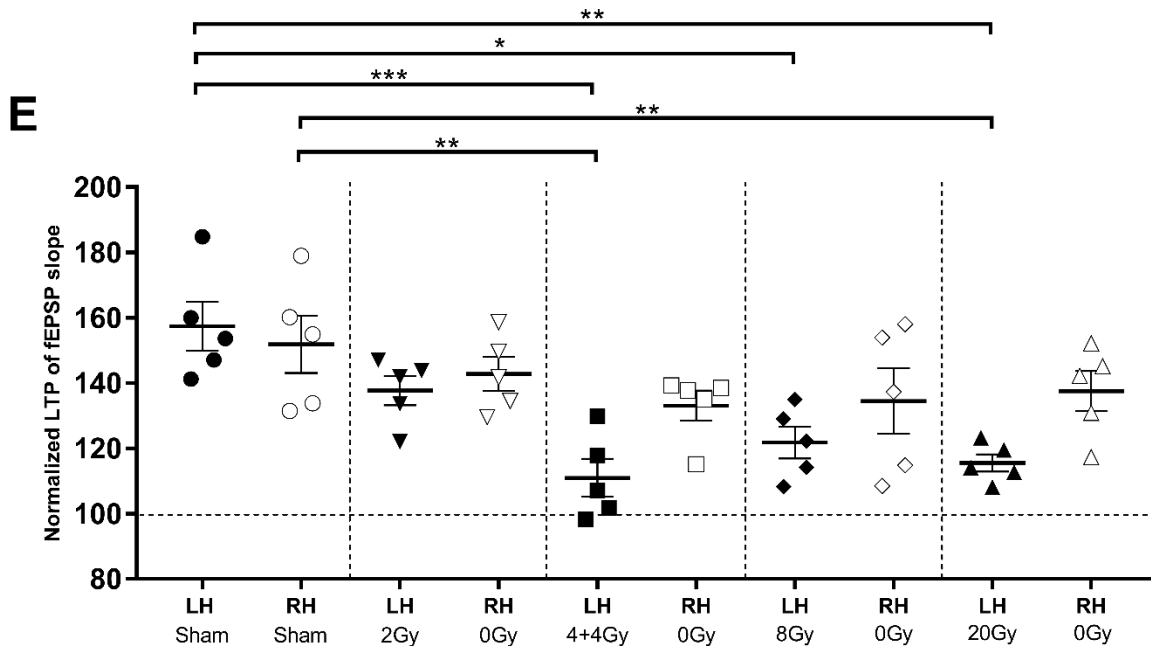


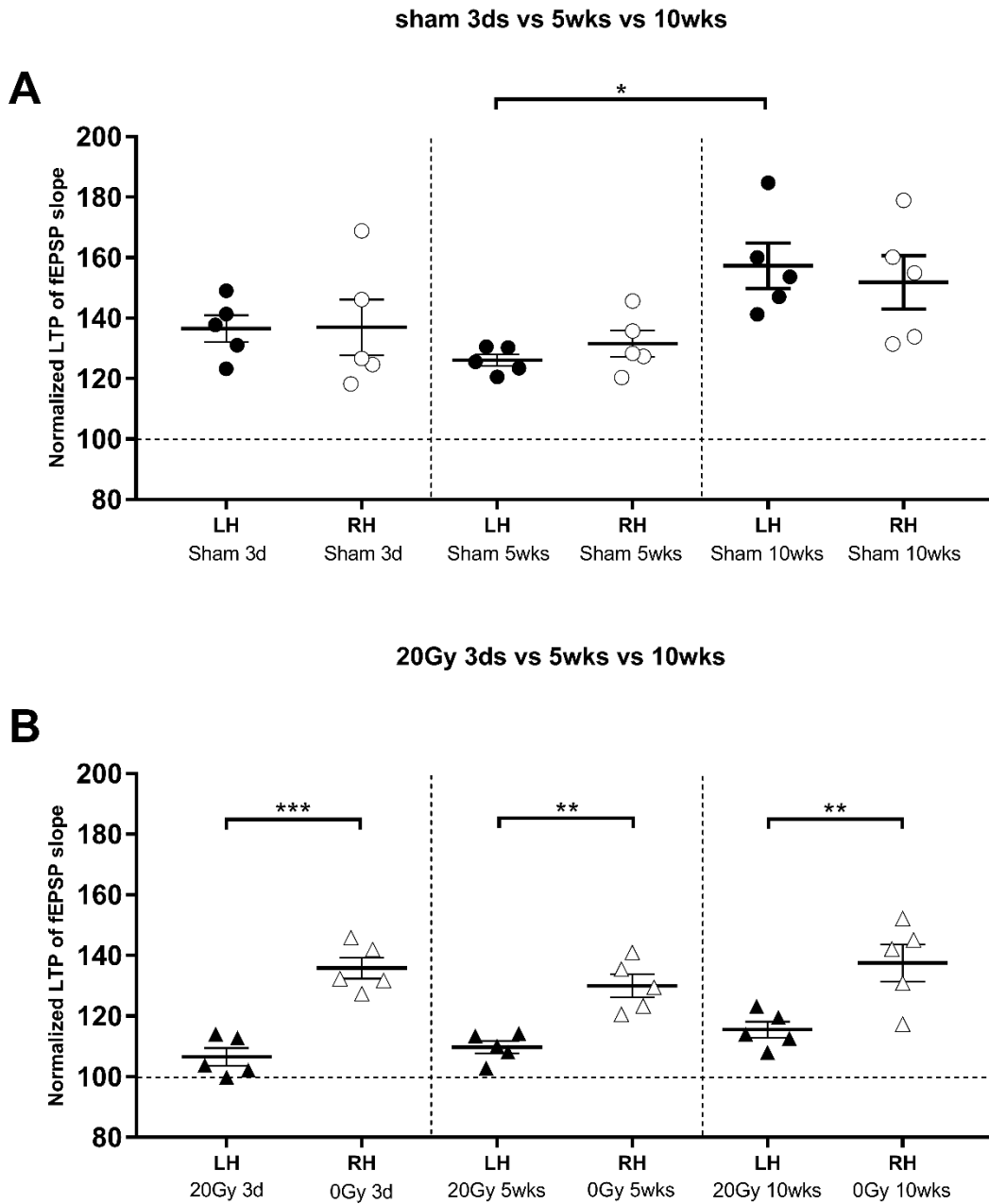
Figure 12. LTP in juvenile mice except 2Gy PBRT remained inhibited 10 weeks after irradiation. 10 weeks after recovery, LTP was measured in left/right hippocampal slices of sham group and irradiated/non-irradiated slices of the RT group at (A) single dose of 20Gy, (B) fractionated dose of 4+4Gy, (C) single dose of 8Gy and (D) single dose of 2Gy. (E) Scatter plot showing the average values of the last 10mins of LTP. 157.3%±2.3% and 151.8%±2.6% (relative to baseline) of sham groups, 137.7%±1.4% and 142.7%±1.6% after 2Gy, 110.9%±1.8% and 133.0%±1.7% after 4+4Gy, 121.7%±1.4% and 134.5%±2.9% after 8Gy, 115.5%±1.0% and 137.9%±1.8% after 20Gy (5 mice per group), respectively. Analysis of LTP in sham and 4+4Gy groups [$F_{(3,16)}=9.32$, $P=0.0008$], 20Gy groups [$F_{(3,16)}=7.78$, $P=0.002$] and

8Gy [$F_{(3,16)}=4.12$, $P=0.0241$] revealed significant differences, however, no significant differences in 2Gy groups [$F_{(3,16)}=1.71$, $P=0.2050$] were detected. LTP remained blocked in 4+4Gy groups (110.9%±1.8%, $P=0.0011$ vs. LH Sham; $P=0.0034$ vs. RH Sham), 8Gy groups (121.7%±1.4%, $P=0.0293$ vs. LH Sham; $P=0.0741$ vs. RH Sham) and 20Gy groups (115.5%±1.0%, $P=0.0022$ vs. LH Sham; $P=0.0071$ vs. RH Sham). LTP in non-irradiated hippocampal slices remained baseline level throughout the different dose regimen: 2Gy groups (142.7%±1.6%, $P=0.8318$ vs. LH Sham; $P=0.9901$ vs. RH Sham), 4+4Gy groups (133.0%±1.7%, $P=0.0990$ vs. LH Sham; $P=0.2549$ vs. RH Sham), 8Gy groups (134.5%±2.9%, $P=0.2256$ vs. LH Sham; $P=0.4458$ vs. RH Sham) and 20Gy groups (137.9%±1.8%, $P=0.1971$ vs. LH Sham; $P=0.4525$ vs. RH Sham) were detected during this period. * $P<0.05$ vs. sham groups.

3.5 Radiation affects LTP dose- and time-dependent

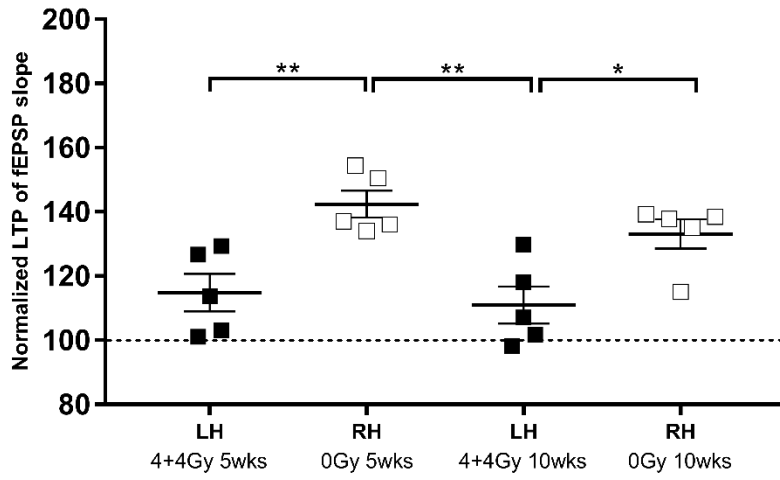
We also investigated if radiation-induced inhibition of LTP dose-dependently over recovery time (Figure 13). No changes in the LTP were observed in sham treated mice [$F_{(5,24)}=3.339$, $P=0.0198$] (Fig. 13A). However, compared with the non-irradiated hippocampus (RH 0Gy), significant differences in the LTP values after a fractionated LH 4+4Gy [$F_{(3,16)}=8.434$, $P=0.0014$] and a single high dose (LH 20Gy)

radiation [$F_{(5,24)}=13.37$, $P<0.0001$] were observed. In contrast, no significant negative effects on LTP were detected in juvenile mice whose LH was irradiated with 8Gy [$F_{(3,16)}=2.464$, $P=0.0998$] or 2Gy [$F_{(3,16)}=0.391$, $P=0.7611$].



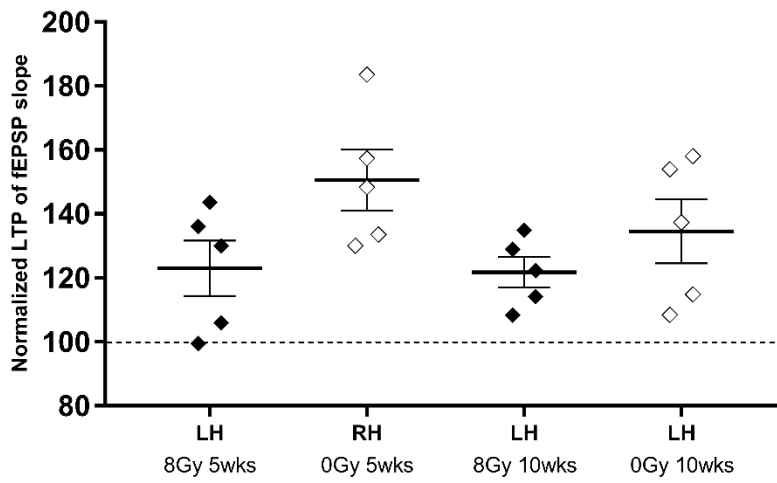
4+4Gy 5wks vs 10wks

C



8Gy 5wks vs 10wks

D



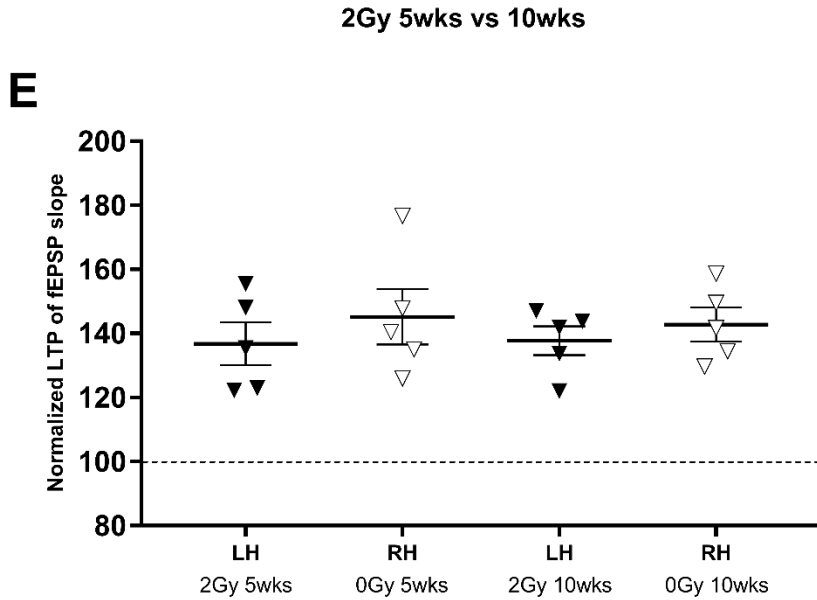


Figure 13. Fractionated 4+4Gy and 20Gy high single dose radiation inhibit LTP. (A) LTP was not influenced by sham irradiation [$F_{(5,24)}=3.339$, $P=0.0198$]. (B), (C) LTP in irradiated hippocampal slices at 5 and 10 weeks was significantly decreased by 20Gy ($P=0.0001$, LH vs. RH 20Gy 3 days; $P=0.0092$, LH vs. RH 20Gy 5 weeks; $P=0.0040$, LH vs. RH 20Gy 10 weeks) and 4+4Gy ($P=0.0078$, LH vs. RH 4+4Gy 5 weeks; $P=0.0350$, LH vs. RH 4+4Gy 10 weeks) irradiation (versus non-irradiated controls). (D) (E) In contrast to non-irradiated hippocampal slices, 8Gy had no significant negative effect on LTP [$F_{(3,16)}=2.464$, $P=0.0998$] or 2Gy [$F_{(3,16)}=0.391$, $P=0.7611$].

3.6 Effects of different dose regimen on body weight of juvenile mice

None of the PBRT doses had any significant effect on the body weight of the juvenile mice 5 and 10 weeks after irradiation, thereby indicating the absence of severe side effects (Figure 14).

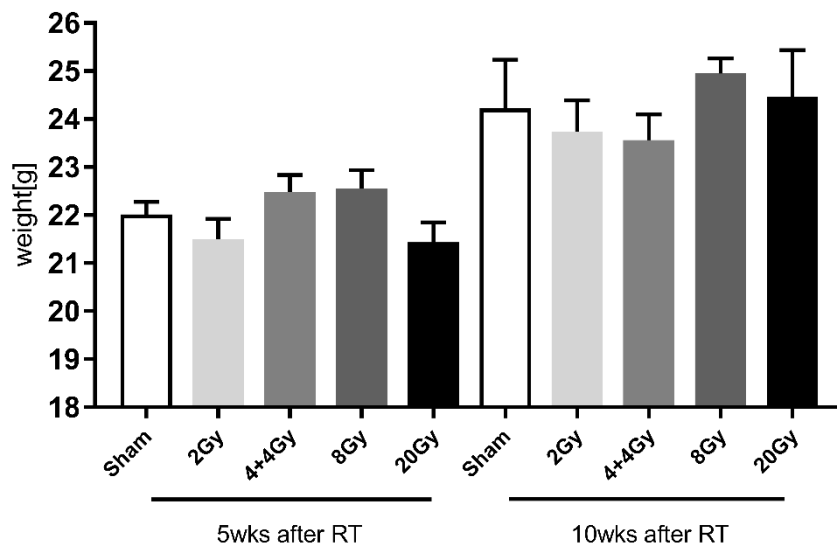


Figure 14. The histograms of effects of different doses on mice body weight.

Body-weight histograms demonstrated there was no difference in body weight among the varying doses of RT groups after 5 weeks [$F_{(4,20)}=2.037, P=0.1278$] or 10 weeks [$F_{(4,20)}=0.5641, P=0.6915$].

3.7 Quantitative hippocampus microvasculature network analysis

The novel EMOVI technique was used to quantify the effects of a PBRT on the microvasculature of the hippocampus. The principle of the measurements is based on the translation of fluorescence data derived from stained vessels (using the endothelial cell marker CD31) in an optically cleared hippocampus into volumetric, representative surfaces. In a second step, two identically sized regions of interest (ROI) were selected to avoid interference in the measurements induced by neurons and large vessels (Fig. 15A and 15C). Looped structures are transferred into a binarized fluorescence signal to automatically trace the vessel path as quantifiable filament objects (Fig. 15B and 15D). EMOVI analyzes the vascular network of the left irradiated (LH 8Gy, LH 20Gy) and right non-irradiated (RH 0Gy) hippocampus of juvenile mice. CD31 staining showed a significant decline in the microvessel density after radiation, especially in the left irradiated hippocampus (LH 20Gy) radiation group after 10 weeks, as compared to the non-irradiated right hippocampus (RH) group ($P=0.0141$) (Fig. 16A). The number of branching points in the LH was lower than the RH groups, 5 and 10 weeks after irradiation with 20Gy (Fig. 16B).

Although not significant, a similar trend was observed for the microvessel length and the branching points in 8Gy radiated mice after 10 weeks (Fig. 16C and 16D). Compared to mice irradiated with 20Gy after 10 weeks, less microvasculature damage was detected in groups of mice which were irradiated with 8Gy. The decline of the branching points and microvessel length indicates a diminished complexity of the microvascular network with less vessels branching and looping.

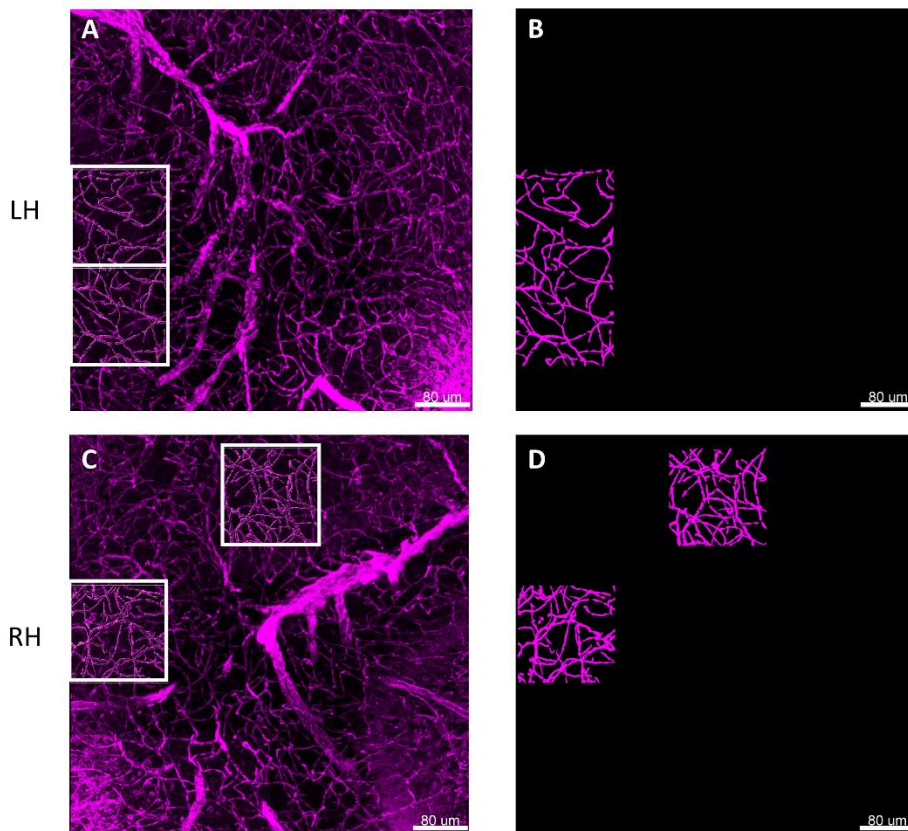
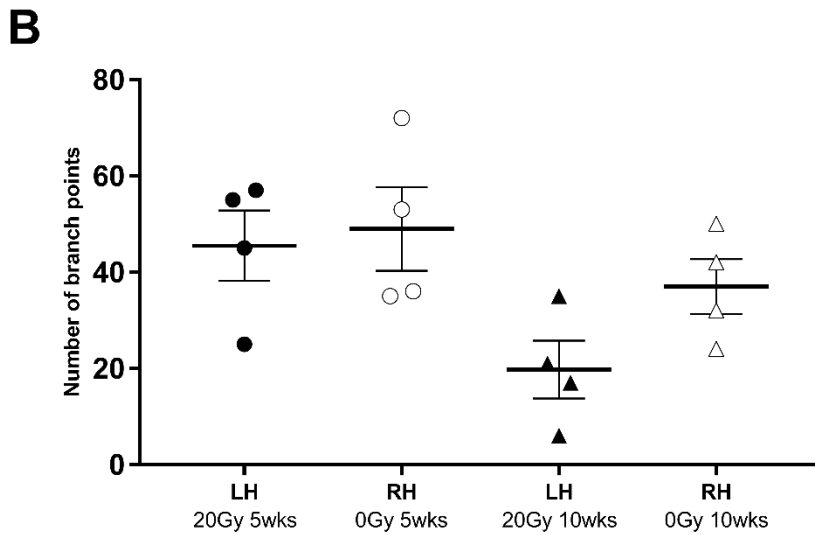
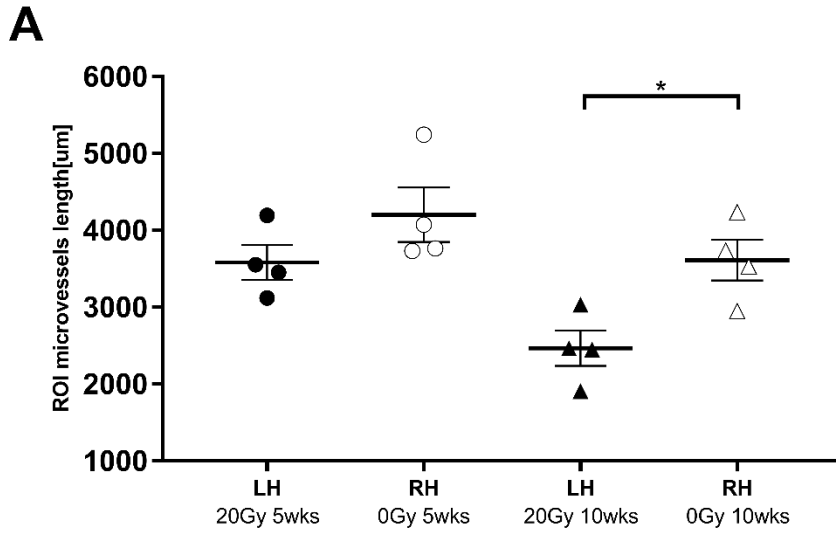


Figure 15. Efficient tissue clearing and multi-organ volumetric imaging. Region of interest (ROI) of left irradiated (A) and right non-irradiated (C) hippocampus

microvasculature treated with 20 Gy PBRT after 10 weeks. (B) (D) The binary masking of the vessel structure is the basis for vessel length and branch detection.



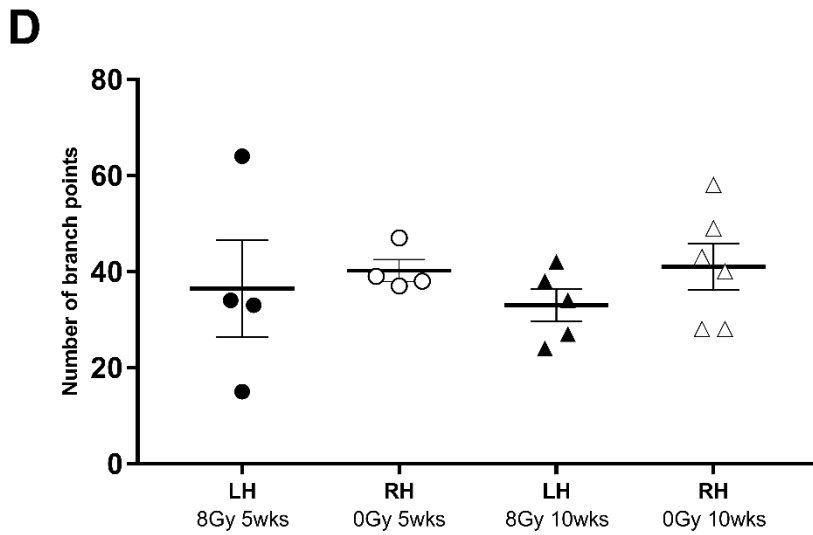
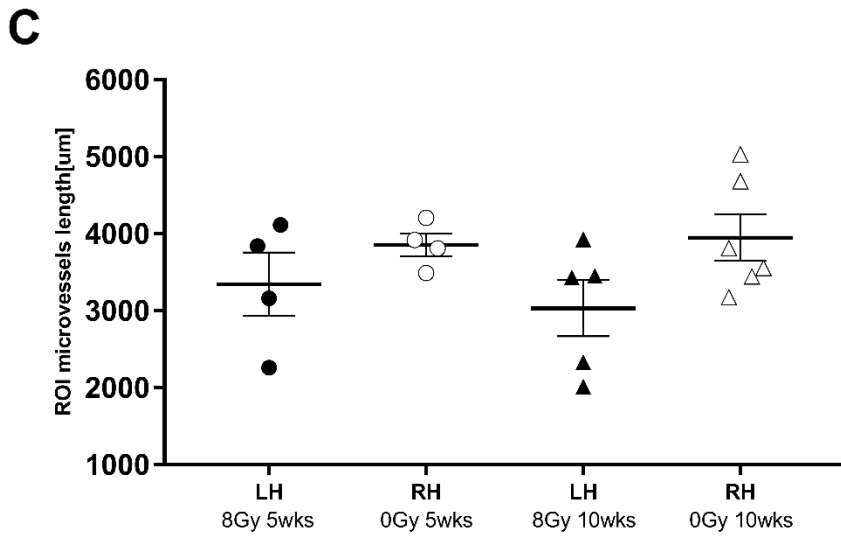


Figure 16. Quantitative vessel network analysis reveals significant loss in hippocampus following targeted PBRT. For the statistical analysis, 2 regions of interest (ROI) with the same area were selected for analysis to avoid the interference of neurons and large vessel datasets. (A) 20Gy PBRT induced a

significant reduction in microvessel length after 10 weeks ($P=0.0141$). (B) After 20Gy PBRT, the number of branch points in the LH (irradiated) hippocampus after 10 weeks was lower than that of the LH (irradiated) and RH (non-irradiated) hippocampus after 5 weeks and was also lower than the RH (non-irradiated) hippocampus after 10 weeks. In contrast, reductions in the length (C) and branch points (D) of microvessels after 8Gy irradiation after 5 weeks and 10 weeks were less than those after 20Gy irradiation.

4. Discussion

Herein, we found that the PBRT-induced inhibition of CA1-LTP in the ipsilateral hippocampus of juvenile mice was dependent on dose and recovery time, while the corresponding contralateral non-irradiated hippocampus remained completely unaffected. Low dose radiation with 2Gy had no negative effects on the LTP. Irradiation-induced inhibition of LTP was associated with a loss in the microvascular network. Although the mechanisms underlying the synaptic alterations need to be studied in more detail, this is the first study providing evidence that PBRT reduces LTP in the hippocampus of juvenile mice only on the ipsilateral irradiated but not on the corresponding non-irradiated contralateral hippocampus. Moreover, even 10 weeks after irradiation no recovery from radiation-induced cognitive function deficits was observed in the irradiated left hippocampus.

Most studies measuring radiation-induced cognitive deficits in neuronal functions have focused on the expression of immediate-early gene activity-regulated cytoskeleton-associated proteins,(Rosi et al., 2008) NMDA receptor subunits(Grosshans et al., 2002) and changes in the hippocampal synaptic strength(Snyder et al., 2001) and either used WBRT animal models(Balentova et al., 2018; Duman et al., 2018; Feng et al., 2018; Parihar & Limoli, 2013; Rola et al., 2004;

D. Zhang et al., 2018) or an ex vivo hippocampal slice radiation.(Wu et al., 2012) However, studies in animal models following PBRT which better reflect the clinical situation have not been reported. Since the developing young brain(Blomstrand et al., 2014; Fukuda et al., 2005; Rola et al., 2004; Roman & Sperduto, 1995; Zanni, Zhou, et al., 2015) is more vulnerable to radiation-induced damage, it is necessary to study radiation effects in young animals.

Our novel findings provide unique evidence for a physiological impairment in unilateral hippocampi induced by fractionated and single dose PBRT. In line with a recent study(D. Zhang et al., 2018) showing acute phase LTP changes in cortical synaptic plasticity after ex vivo irradiation of hippocampus slices with 10Gy, we demonstrate a radiation-induced decrease in LTP on day 3 after PBRT with 20Gy. Similar to other studies radiation-induced LTP inhibition was still present 10 weeks after irradiation. This long-term sustained disability of LTP induction corresponds to late radiation-induced effects in humans which are most pronounced in immature brains.(Fukuda et al., 2005) Other studies(Madsen et al., 2003; Rola et al., 2004; D. Zhang et al., 2018) have suggested that WBRT-induced long-term impairment of dentate SGZ neurogenesis in young mice is associated with deficits in hippocampus-dependent memory. In the hippocampal-PFC circuit, LTP inhibition lasted for 5 months after WBRT when juvenile rats were irradiated.(D. Zhang et al.,

2018) Strikingly, in the present study PBRT did not produce an LTP impairment in the non-irradiated hippocampus even after a single high-dose radiation. More recently, the prevailing feeling is that patients receiving fractionated partial or WBRT can develop significant CI later than 6 months after irradiation.(Greene-Schloesser & Robbins, 2012) Recently, a phase III clinical trial demonstrated that a pre-treatment of the hippocampus with memantine during WBRT effectively preserved cognitive functions and patient-reported symptoms.(P. D. Brown et al., 2020) Our observations demonstrate different LTP changes after PBRT in the ipsilateral and contralateral hippocampus. Additionally, Giulia Zanni et al. have shown that the application of WBRT to juvenile rats on postnatal day 11 resulted in long-term alterations and HFS delivery in the DG that no longer produces LTP, but promotes a shift to long-term depression.(Zanni, Zhou, et al., 2015) Although LTP recovered slowly within 8 weeks after WBRT in adult rats(D. Zhang et al., 2018), irradiation of the juvenile brains caused irreversible deficits in synaptic plasticity. These data suggest that different mechanisms are involved in degenerative as well as regenerative processes after juvenile and adult hippocampi were treated with radiation. A possible explanation for the severe impairment of juvenile brains after RT could be a massive apoptosis of stem cells in combination with an impaired production of growth factors that result in a massive decline in cells with the

capacity to proliferate.(Blomstrand et al., 2014; Fukuda et al., 2005; Roughton et al., 2013; Schindler et al., 2008)

Interestingly, in our study a fractionated dose of 4+4Gy was more deleterious on LTP than a single dose with 8Gy after a recovery of 5 and 10 weeks after PBRT. Zoé Schmal et al. reported that hippocampal neurogenesis is highly sensitive to repetitive fractionated low irradiation doses which induce an accumulation of DNA damage and thereby compromise hippocampal neurogenesis.(Schmal et al., 2019)

A recent study confirmed that fractionated radiation-induced CI is closely related to accelerated neuronal cell death, inhibition of neurogenesis, activation of astrocytes and microglia and an early induction of radiation-induced damage.(Balentova et al., 2018) It also has been shown that both, a single, high dose of WBRT(Ljubimova et al., 1991) as well as a cumulative fractionated application at low doses(W. R. Brown et al., 2005) can impair the microvasculature of the brain. Within the CA1 region of the hippocampus, a reduction in the endothelial cells was induced 12 months after single doses as low as 0.5Gy and 2Gy.(Mao et al., 2010) In our study, a PBRT with 20Gy after 10 weeks was found to induce more damage in the microvasculature than a dose of 8Gy after 10 weeks.

In our study, a conventional fractionated PBRT given at 2Gy to juvenile mice did not reduce LTP at any measured time point. This finding is in accordance with the findings of others showing no spatial learning and memory deficits in mice 2 months after exposure to a single WBRT dose of 2Gy.(Dulcich & Hartman, 2013) Although WBRT with 1.0 or 1.5Gy has been reported to seriously reduce body weight of mice at an age of 6 weeks,(Sun et al., 1994) we did not detect any significant effect on body weight 5 and 10 weeks after irradiation. Another study showed that a combined treatment consisting of split-dose (total cumulative doses: 3.0, 4.0, 5.1Gy) ionizing radiation and chronic magnetic field exposure at an early age can result in an increased body weight.(Babbitt et al., 2001) Taken together, although the mechanisms underlying the synaptic alterations need to be further elucidated, our findings provide a more detailed understanding of how PBRT impacts on the bilateral hippocampi of juvenile mice. Our preclinical results might help to design protective strategies to rescue the young developing brain from cognitive decline by PBRT.

Nonetheless, these results must be interpreted with caution and potential limitations should be kept in mind. One major drawback of this study is that although we try to simulate the clinical RT treatment plan, this study was performed on a selective dose regimen that may limit the generalization of the

findings. Future studies are required to determine different clinical related dose effects on the brain of animals and on human cognitive functions after irradiation of children at different ages. We also have to point out that strictly executed randomized trials with larger animal cohorts are necessary. It may give rise to bias under single-blind conditions when we evaluate the hippocampal microvasculature changes.

In conclusion, this study presents the first evidence that PBRT induces both, microvascular and LTP impairment in the juvenile hippocampal CA1 region. And that this damage is restricted to the irradiated hippocampus, while the corresponding non-irradiated, contralateral hippocampus remained unaffected. Although we assumed that the non-irradiated hippocampus may also be influenced by irradiation we could not determine any defects in the non-irradiated part of the hippocampus. Also compensatory effects of the non-irradiated part of the hippocampus were not observed up to 10 and 20 weeks after irradiation, although the left and right hippocampus are connected. Our findings also indicate that a treatment of juvenile mouse brains with fractionated radiation doses is more deleterious with respect to the LTP than a single dose. This differential effect in the bilateral hippocampus may contribute to radiation-induced CI in juvenile rodents as well as in children. Since RT with hippocampal avoidance is feasible in patients(P.

D. Brown et al., 2020; Gondi, Tome, et al., 2010) and rats,(Cramer et al., 2015) it is essential to consider radiation-induced cognitive deficits on juvenile brains. Further studies elucidating the potential mechanisms with respect to synaptic plasticity alterations are likely to improve RT plans and the QOL of pediatric patients.

5. Summary

Radiation is the first-line therapy for both primary and metastatic CNS tumors. However, radiation-induced cognitive deficits are a major concern, especially in pediatric brain tumor patients. Although previous preclinical studies investigated the hippocampus after WBRT, these do not closely reflect the clinical situation. Furthermore, the mechanisms of cognitive ipsilateral and contralateral changes in the hippocampus after PBRT of juvenile mice have not been investigated in detail. Herein, we demonstrate that PBRT induces a long-lasting inhibition of LTP in the irradiated hippocampal CA1 region, whereas the contralateral, non-irradiated hippocampus remained completely unaffected. Irradiation-induced LTP inhibition was associated with a significant loss in the microvascular network. Our findings on the PBRT-induced impairment of the bilateral hippocampi in juvenile mice could help to design protective strategies to rescue the young developing brain of children from cognitive decline after RT.

6. References

- Acharya, M. M., Christie, L. A., Lan, M. L., Giedzinski, E., Fike, J. R., Rosi, S., & Limoli, C. L. (2011). Human neural stem cell transplantation ameliorates radiation-induced cognitive dysfunction. *Cancer Res*, *71*(14), 4834-4845. doi:10.1158/0008-5472.CAN-11-0027
- Amini, P., Mirtavoos-Mahyari, H., Motevaseli, E., Shabeeb, D., Musa, A. E., Cheki, M., Farhood, B., Yahyapour, R., Shirazi, A., Goushbolagh, N. A., & Najafi, M. (2019). Mechanisms for Radioprotection by Melatonin; Can it be Used as a Radiation Countermeasure? *Curr Mol Pharmacol*, *12*(1), 2-11. doi:10.2174/1874467211666180802164449
- Artola, A., & Singer, W. (1993). Long-term depression of excitatory synaptic transmission and its relationship to long-term potentiation. *Trends Neurosci*, *16*(11), 480-487. doi:10.1016/0166-2236(93)90081-v
- Attia, A., Page, B. R., Lesser, G. J., & Chan, M. (2014). Treatment of radiation-induced cognitive decline. *Curr Treat Options Oncol*, *15*(4), 539-550. doi:10.1007/s11864-014-0307-3
- Babbitt, J. T., Kharazi, A. I., Taylor, J. M., Bonds, C. B., Zhuang, D., Mirell, S. G., Frumkin, E., & Hahn, T. J. (2001). Increased body weight in C57BL/6 female mice after exposure to ionizing radiation or 60Hz magnetic fields. *Int J Radiat Biol*, *77*(8), 875-882. doi:10.1080/09553000110055790
- Balentova, S., Hajtmanova, E., Filova, B., Borbelyova, V., Lehotsky, J., & Adamkov, M. (2018). Effects of fractionated whole-brain irradiation on cellular composition and cognitive function in the rat brain. *Int J Radiat Biol*, *94*(3), 238-247. doi:10.1080/09553002.2018.1425805
- Birks, J. S., & Harvey, R. J. (2018). Donepezil for dementia due to Alzheimer's disease. *Cochrane Database Syst Rev*, *6*, CD001190. doi:10.1002/14651858.CD001190.pub3
- Blomstrand, M., Kalm, M., Grander, R., Bjork-Eriksson, T., & Blomgren, K. (2014). Different reactions to irradiation in the juvenile and adult hippocampus. *Int J Radiat Biol*, *90*(9), 807-815. doi:10.3109/09553002.2014.942015
- Briere, M. E., Scott, J. G., McNall-Knapp, R. Y., & Adams, R. L. (2008). Cognitive outcome in pediatric brain tumor survivors: delayed attention deficit at long-term follow-up. *Pediatr Blood Cancer*, *50*(2), 337-340. doi:10.1002/pbc.21223
- Bright, J. J., Kanakasabai, S., Chearwae, W., & Chakraborty, S. (2008). PPAR Regulation of Inflammatory Signaling in CNS Diseases. *PPAR Res*, *2008*, 658520. doi:10.1155/2008/658520
- Brown, P. D., Ballman, K. V., Cerhan, J. H., Anderson, S. K., Carrero, X. W., Whitton, A. C., Greenspoon, J., Parney, I. F., Laack, N. N. I., Ashman, J. B., Bahary, J. P., Hadjipanayis, C. G., Urbanic, J. J., Barker, F. G., 2nd, Farace, E., Khuntia, D., Giannini, C., Buckner, J. C., Galanis, E., & Roberge, D. (2017). Postoperative stereotactic radiosurgery compared with whole brain radiotherapy for resected metastatic brain disease (NCCTG N107C/CEC.3): a multicentre, randomised, controlled, phase 3 trial. *Lancet Oncol*, *18*(8), 1049-1060. doi:10.1016/S1470-2045(17)30441-2
- Brown, P. D., Gondi, V., Pugh, S., Tome, W. A., Wefel, J. S., Armstrong, T. S., Bovi, J. A., Robinson, C., Kanski, A., Khuntia, D., Grosshans, D., Benzinger, T. L. S., Bruner, D., Gilbert, M. R., Roberge, D., Kundapur, V., Devisetty, K., Shah, S., Usuki, K., Anderson, B. M., Stea, B., Yoon, H., Li, J., Laack, N. N., Kruser, T. J., Chmura, S. J., Shi, W., Deshmukh, S., Mehta, M. P., Kachnic, L. A., & for, N. R. G. O. (2020). Hippocampal Avoidance During Whole-Brain Radiotherapy Plus Memantine for Patients With Brain Metastases: Phase III Trial NRG Oncology CC001. *J Clin Oncol*, *38*(10), 1019-1029. doi:10.1200/JCO.19.02767
- Brown, P. D., Jaeckle, K., Ballman, K. V., Farace, E., Cerhan, J. H., Anderson, S. K., Carrero, X. W., Barker, F. G., 2nd, Deming, R., Burri, S. H., Menard, C., Chung, C., Stieber, V. W., Pollock, B. E., Galanis,

- E., Buckner, J. C., & Asher, A. L. (2016). Effect of Radiosurgery Alone vs Radiosurgery With Whole Brain Radiation Therapy on Cognitive Function in Patients With 1 to 3 Brain Metastases: A Randomized Clinical Trial. *JAMA*, *316*(4), 401-409. doi:10.1001/jama.2016.9839
- Brown, P. D., Pugh, S., Laack, N. N., Wefel, J. S., Khuntia, D., Meyers, C., Choucair, A., Fox, S., Suh, J. H., Roberge, D., Kavadi, V., Bentzen, S. M., Mehta, M. P., Watkins-Bruner, D., & Radiation Therapy Oncology, G. (2013). Memantine for the prevention of cognitive dysfunction in patients receiving whole-brain radiotherapy: a randomized, double-blind, placebo-controlled trial. *Neuro Oncol*, *15*(10), 1429-1437. doi:10.1093/neuonc/not114
- Brown, W. R., Blair, R. M., Moody, D. M., Thore, C. R., Ahmed, S., Robbins, M. E., & Wheeler, K. T. (2007). Capillary loss precedes the cognitive impairment induced by fractionated whole-brain irradiation: a potential rat model of vascular dementia. *J Neurol Sci*, *257*(1-2), 67-71. doi:10.1016/j.jns.2007.01.014
- Brown, W. R., Thore, C. R., Moody, D. M., Robbins, M. E., & Wheeler, K. T. (2005). Vascular damage after fractionated whole-brain irradiation in rats. *Radiat Res*, *164*(5), 662-668. doi:10.1667/rr3453.1
- Calvo, W., Hopewell, J. W., Reinhold, H. S., & Yeung, T. K. (1988). Time- and dose-related changes in the white matter of the rat brain after single doses of X rays. *Br J Radiol*, *61*(731), 1043-1052. doi:10.1259/0007-1285-61-731-1043
- Chakraborti, A., Allen, A., Allen, B., Rosi, S., & Fike, J. R. (2012). Cranial irradiation alters dendritic spine density and morphology in the hippocampus. *PLoS One*, *7*(7), e40844. doi:10.1371/journal.pone.0040844
- Chang, E. L., Wefel, J. S., Hess, K. R., Allen, P. K., Lang, F. F., Kornguth, D. G., Arbuckle, R. B., Swint, J. M., Shiu, A. S., Maor, M. H., & Meyers, C. A. (2009). Neurocognition in patients with brain metastases treated with radiosurgery or radiosurgery plus whole-brain irradiation: a randomised controlled trial. *Lancet Oncol*, *10*(11), 1037-1044. doi:10.1016/S1470-2045(09)70263-3
- Chin, H. W., & Maruyama, Y. (1984). Age at treatment and long-term performance results in medulloblastoma. *Cancer*, *53*(9), 1952-1958. doi:10.1002/1097-0142(19840501)53:9<1952::aid-cncr2820530925>3.0.co;2-x
- Citrin, D. E., Shankavaram, U., Horton, J. A., Shield, W., 3rd, Zhao, S., Asano, H., White, A., Sowers, A., Thetford, A., & Chung, E. J. (2013). Role of type II pneumocyte senescence in radiation-induced lung fibrosis. *J Natl Cancer Inst*, *105*(19), 1474-1484. doi:10.1093/jnci/djt212
- Collingridge, G. L., Kehl, S. J., & McLennan, H. (1983). Excitatory amino acids in synaptic transmission in the Schaffer collateral-commissural pathway of the rat hippocampus. *J Physiol*, *334*, 33-46. doi:10.1113/jphysiol.1983.sp014478
- Contestabile, A., Greco, B., Ghezzi, D., Tucci, V., Benfenati, F., & Gasparini, L. (2013). Lithium rescues synaptic plasticity and memory in Down syndrome mice. *J Clin Invest*, *123*(1), 348-361. doi:10.1172/JCI64650
- Cooke, S. F., & Bliss, T. V. (2006). Plasticity in the human central nervous system. *Brain*, *129*(Pt 7), 1659-1673. doi:10.1093/brain/awl082
- Coppe, J. P., Desprez, P. Y., Krtolica, A., & Campisi, J. (2010). The senescence-associated secretory phenotype: the dark side of tumor suppression. *Annu Rev Pathol*, *5*, 99-118. doi:10.1146/annurev-pathol-121808-102144
- Cramer, C. K., Yoon, S. W., Reinsvold, M., Joo, K. M., Norris, H., Hood, R. C., Adamson, J. D., Klein, R. C., Kirsch, D. G., & Oldham, M. (2015). Treatment Planning and Delivery of Whole Brain Irradiation with Hippocampal Avoidance in Rats. *PLoS One*, *10*(12), e0143208. doi:10.1371/journal.pone.0143208

- Crossen, J. R., Garwood, D., Glatstein, E., & Neuwelt, E. A. (1994). Neurobehavioral sequelae of cranial irradiation in adults: a review of radiation-induced encephalopathy. *J Clin Oncol*, *12*(3), 627-642. doi:10.1200/JCO.1994.12.3.627
- Danysz, W., Parsons, C. G., Karcz-Kubicha, M., Schwaier, A., Popik, P., Wedzony, K., Lazarewicz, J., & Quack, G. (1998). GlycineB antagonists as potential therapeutic agents. Previous hopes and present reality. *Amino Acids*, *14*(1-3), 235-239. doi:10.1007/BF01345268
- Duffner, P. K., Cohen, M. E., Voorhess, M. L., MacGillivray, M. H., Brecher, M. L., Panahon, A., & Gilani, B. B. (1985). Long-term effects of cranial irradiation on endocrine function in children with brain tumors. A prospective study. *Cancer*, *56*(9), 2189-2193. doi:10.1002/1097-0142(19851101)56:9<2189::aid-cncr2820560909>3.0.co;2-i
- Dulcich, M. S., & Hartman, R. E. (2013). Pomegranate supplementation improves affective and motor behavior in mice after radiation exposure. *Evid Based Complement Alternat Med*, *2013*, 940830. doi:10.1155/2013/940830
- Duman, J. G., Dinh, J., Zhou, W., Cham, H., Mavratsas, V. C., Paveskovic, M., Mulherkar, S., McGovern, S. L., Tolia, K. F., & Grosshans, D. R. (2018). Memantine prevents acute radiation-induced toxicities at hippocampal excitatory synapses. *Neuro Oncol*, *20*(5), 655-665. doi:10.1093/neuonc/nox203
- Estrada, H., Rebling, J., Sievert, W., Hladik, D., Hofmann, U., Gottschalk, S., Tapio, S., Multhoff, G., & Razansky, D. (2020). Intravital optoacoustic and ultrasound bio-microscopy reveal radiation-inhibited skull angiogenesis. *Bone*, *133*, 115251. doi:10.1016/j.bone.2020.115251
- Fagiolini, M., & Hensch, T. K. (2000). Inhibitory threshold for critical-period activation in primary visual cortex. *Nature*, *404*(6774), 183-186. doi:10.1038/35004582
- Farhood, B., Goradel, N. H., Mortezaee, K., Khanlarkhani, N., Salehi, E., Nashtaei, M. S., Mirtavoos-Mahyari, H., Motevaseli, E., Shabeeb, D., Musa, A. E., & Najafi, M. (2019). Melatonin as an adjuvant in radiotherapy for radioprotection and radiosensitization. *Clin Transl Oncol*, *21*(3), 268-279. doi:10.1007/s12094-018-1934-0
- Feng, X., Liu, S., Chen, D., Rosi, S., & Gupta, N. (2018). Rescue of cognitive function following fractionated brain irradiation in a novel preclinical glioma model. *Elife*, *7*. doi:10.7554/eLife.38865
- FitzGerald, D. B., Crucian, G. P., Mielke, J. B., Shenal, B. V., Burks, D., Womack, K. B., Ghacibeh, G., Drago, V., Foster, P. S., Valenstein, E., & Heilman, K. M. (2008). Effects of donepezil on verbal memory after semantic processing in healthy older adults. *Cogn Behav Neurol*, *21*(2), 57-64. doi:10.1097/WNN.0b013e3181799df1
- Fountoulakis, K. N., Vieta, E., Sanchez-Moreno, J., Kaprinis, S. G., Goikolea, J. M., & Kaprinis, G. S. (2005). Treatment guidelines for bipolar disorder: a critical review. *J Affect Disord*, *86*(1), 1-10. doi:10.1016/j.jad.2005.01.004
- Fukuda, A., Fukuda, H., Swanpalmer, J., Hertzman, S., Lannering, B., Marky, I., Bjork-Eriksson, T., & Blomgren, K. (2005). Age-dependent sensitivity of the developing brain to irradiation is correlated with the number and vulnerability of progenitor cells. *J Neurochem*, *92*(3), 569-584. doi:10.1111/j.1471-4159.2004.02894.x
- Fukui, M., Choi, H. J., & Zhu, B. T. (2010). Mechanism for the protective effect of resveratrol against oxidative stress-induced neuronal death. *Free Radic Biol Med*, *49*(5), 800-813. doi:10.1016/j.freeradbiomed.2010.06.002
- Fukui, M., & Zhu, B. T. (2010). Mitochondrial superoxide dismutase SOD2, but not cytosolic SOD1, plays a critical role in protection against glutamate-induced oxidative stress and cell death in HT22 neuronal cells. *Free Radic Biol Med*, *48*(6), 821-830. doi:10.1016/j.freeradbiomed.2009.12.024
- Gage, F. H. (2000). Mammalian neural stem cells. *Science*, *287*(5457), 1433-1438. doi:10.1126/science.287.5457.1433

- Giovagnoli, A. R., & Boiardi, A. (1994). Cognitive impairment and quality of life in long-term survivors of malignant brain tumors. *Ital J Neurol Sci*, *15*(9), 481-488. doi:10.1007/BF02334609
- Gondi, V., Hermann, B. P., Mehta, M. P., & Tome, W. A. (2012). Hippocampal dosimetry predicts neurocognitive function impairment after fractionated stereotactic radiotherapy for benign or low-grade adult brain tumors. *Int J Radiat Oncol Biol Phys*, *83*(4), e487-493. doi:10.1016/j.ijrobp.2011.10.021
- Gondi, V., Pugh, S. L., Tome, W. A., Caine, C., Corn, B., Kanner, A., Rowley, H., Kundapur, V., DeNittis, A., Greenspoon, J. N., Konski, A. A., Bauman, G. S., Shah, S., Shi, W., Wendland, M., Kachnic, L., & Mehta, M. P. (2014). Preservation of memory with conformal avoidance of the hippocampal neural stem-cell compartment during whole-brain radiotherapy for brain metastases (RTOG 0933): a phase II multi-institutional trial. *J Clin Oncol*, *32*(34), 3810-3816. doi:10.1200/JCO.2014.57.2909
- Gondi, V., Tolakanahalli, R., Mehta, M. P., Tewatia, D., Rowley, H., Kuo, J. S., Khuntia, D., & Tome, W. A. (2010). Hippocampal-sparing whole-brain radiotherapy: a "how-to" technique using helical tomotherapy and linear accelerator-based intensity-modulated radiotherapy. *Int J Radiat Oncol Biol Phys*, *78*(4), 1244-1252. doi:10.1016/j.ijrobp.2010.01.039
- Gondi, V., Tome, W. A., & Mehta, M. P. (2010). Why avoid the hippocampus? A comprehensive review. *Radiother Oncol*, *97*(3), 370-376. doi:10.1016/j.radonc.2010.09.013
- Greene-Schloesser, D., Moore, E., & Robbins, M. E. (2013). Molecular pathways: radiation-induced cognitive impairment. *Clin Cancer Res*, *19*(9), 2294-2300. doi:10.1158/1078-0432.CCR-11-2903
- Greene-Schloesser, D., & Robbins, M. E. (2012). Radiation-induced cognitive impairment--from bench to bedside. *Neuro Oncol*, *14 Suppl 4*, iv37-44. doi:10.1093/neuonc/nos196
- Greene-Schloesser, D., Robbins, M. E., Peiffer, A. M., Shaw, E. G., Wheeler, K. T., & Chan, M. D. (2012). Radiation-induced brain injury: A review. *Front Oncol*, *2*, 73. doi:10.3389/fonc.2012.00073
- Gron, G., Kirstein, M., Thielscher, A., Riepe, M. W., & Spitzer, M. (2005). Cholinergic enhancement of episodic memory in healthy young adults. *Psychopharmacology (Berl)*, *182*(1), 170-179. doi:10.1007/s00213-005-0043-2
- Grosshans, D. R., Clayton, D. A., Coultrap, S. J., & Browning, M. D. (2002). LTP leads to rapid surface expression of NMDA but not AMPA receptors in adult rat CA1. *Nat Neurosci*, *5*(1), 27-33. doi:10.1038/nn779
- Guillen, J. (2012). FELASA guidelines and recommendations. *J Am Assoc Lab Anim Sci*, *51*(3), 311-321. Retrieved from <https://www.ncbi.nlm.nih.gov/pubmed/22776188>
- Gutierrez, A. N., Westerly, D. C., Tome, W. A., Jaradat, H. A., Mackie, T. R., Bentzen, S. M., Khuntia, D., & Mehta, M. P. (2007). Whole brain radiotherapy with hippocampal avoidance and simultaneously integrated brain metastases boost: a planning study. *Int J Radiat Oncol Biol Phys*, *69*(2), 589-597. doi:10.1016/j.ijrobp.2007.05.038
- Haldbo-Classen, L., Amidi, A., Lukacova, S., Wu, L. M., Oettingen, G. V., Lassen-Ramshad, Y., Zachariae, R., Kallehauge, J. F., & Hoyer, M. (2020). Cognitive impairment following radiation to hippocampus and other brain structures in adults with primary brain tumours. *Radiother Oncol*, *148*, 1-7. doi:10.1016/j.radonc.2020.03.023
- Harth, S., Abo-Madyan, Y., Zheng, L., Siebenlist, K., Herskind, C., Wenz, F., & Giordano, F. A. (2013). Estimation of intracranial failure risk following hippocampal-sparing whole brain radiotherapy. *Radiother Oncol*, *109*(1), 152-158. doi:10.1016/j.radonc.2013.09.009
- Haussler, U., Rinas, K., Kiliyas, A., Egert, U., & Haas, C. A. (2016). Mossy fiber sprouting and pyramidal cell dispersion in the hippocampal CA2 region in a mouse model of temporal lobe epilepsy. *Hippocampus*, *26*(5), 577-588. doi:10.1002/hipo.22543
- Hayyan, M., Hashim, M. A., & AlNashef, I. M. (2016). Superoxide Ion: Generation and Chemical Implications. *Chem Rev*, *116*(5), 3029-3085. doi:10.1021/acs.chemrev.5b00407

- Hellstrom, N. A., Bjork-Eriksson, T., Blomgren, K., & Kuhn, H. G. (2009). Differential recovery of neural stem cells in the subventricular zone and dentate gyrus after ionizing radiation. *Stem Cells*, 27(3), 634-641. doi:10.1634/stemcells.2008-0732
- Hellstrom, N. A., Lindberg, O. R., Stahlberg, A., Swanpalmer, J., Pekny, M., Blomgren, K., & Kuhn, H. G. (2011). Unique gene expression patterns indicate microglial contribution to neural stem cell recovery following irradiation. *Mol Cell Neurosci*, 46(4), 710-719. doi:10.1016/j.mcn.2011.02.001
- Hinkle, J. J., Olschowka, J. A., Love, T. M., Williams, J. P., & O'Banion, M. K. (2019). Cranial irradiation mediated spine loss is sex-specific and complement receptor-3 dependent in male mice. *Sci Rep*, 9(1), 18899. doi:10.1038/s41598-019-55366-6
- Hochberg, F. H., & Pruitt, A. (1980). Assumptions in the radiotherapy of glioblastoma. *Neurology*, 30(9), 907-911. doi:10.1212/wnl.30.9.907
- Hofmann, J., Gadjalova, I., Mishra, R., Ruland, J., & Keppler, S. J. (2020). Efficient Tissue Clearing and Multi-Organ Volumetric Imaging Enable Quantitative Visualization of Sparse Immune Cell Populations During Inflammation. *Front Immunol*, 11, 599495. doi:10.3389/fimmu.2020.599495
- Hong, J. H., Chiang, C. S., Campbell, I. L., Sun, J. R., Withers, H. R., & McBride, W. H. (1995). Induction of acute phase gene expression by brain irradiation. *Int J Radiat Oncol Biol Phys*, 33(3), 619-626. doi:10.1016/0360-3016(95)00279-8
- Hopewell, J. W., & Wright, E. A. (1970). The nature of latent cerebral irradiation damage and its modification by hypertension. *Br J Radiol*, 43(507), 161-167. doi:10.1259/0007-1285-43-507-161
- Hunt, C. R., Ramnarain, D., Horikoshi, N., Iyengar, P., Pandita, R. K., Shay, J. W., & Pandita, T. K. (2013). Histone modifications and DNA double-strand break repair after exposure to ionizing radiations. *Radiat Res*, 179(4), 383-392. doi:10.1667/RR3308.2
- Huo, K., Sun, Y., Li, H., Du, X., Wang, X., Karlsson, N., Zhu, C., & Blomgren, K. (2012). Lithium reduced neural progenitor apoptosis in the hippocampus and ameliorated functional deficits after irradiation to the immature mouse brain. *Mol Cell Neurosci*, 51(1-2), 32-42. doi:10.1016/j.mcn.2012.07.002
- Janzer, R. C., & Raff, M. C. (1987). Astrocytes induce blood-brain barrier properties in endothelial cells. *Nature*, 325(6101), 253-257. doi:10.1038/325253a0
- Jenrow, K. A., Liu, J., Brown, S. L., Kolozsvary, A., Lapanowski, K., & Kim, J. H. (2011). Combined atorvastatin and ramipril mitigate radiation-induced impairment of dentate gyrus neurogenesis. *J Neurooncol*, 101(3), 449-456. doi:10.1007/s11060-010-0282-x
- Johannesen, T. B., Lien, H. H., Hole, K. H., & Lote, K. (2003). Radiological and clinical assessment of long-term brain tumour survivors after radiotherapy. *Radiother Oncol*, 69(2), 169-176. doi:10.1016/s0167-8140(03)00192-0
- Johnston, D., & Amaral, D. G. (2004). Hippocampus. In *The synaptic organization of the brain*, 5th ed. (pp. 455-498). New York, NY, US: Oxford University Press.
- Kale, A., Piskin, O., Bas, Y., Aydin, B. G., Can, M., Elmas, O., & Buyukuysal, C. (2018). Neuroprotective effects of Quercetin on radiation-induced brain injury in rats. *J Radiat Res*, 59(4), 404-410. doi:10.1093/jrr/rry032
- Keime-Guibert, F., Chinot, O., Taillandier, L., Cartalat-Carel, S., Frenay, M., Kantor, G., Guillamo, J. S., Jadaud, E., Colin, P., Bondiau, P. Y., Menei, P., Loiseau, H., Bernier, V., Honnorat, J., Barrie, M., Mokhtari, K., Mazon, J. J., Bissery, A., Delattre, J. Y., & Association of French-Speaking, N.-O. (2007). Radiotherapy for glioblastoma in the elderly. *N Engl J Med*, 356(15), 1527-1535. doi:10.1056/NEJMoa065901
- Kiffer, F., Alexander, T., Anderson, J., Groves, T., McElroy, T., Wang, J., Sridharan, V., Bauer, M., Boerma, M., & Allen, A. (2020). Late Effects of (1)H + (16)O on Short-Term and Object Memory, Hippocampal Dendritic Morphology and Mutagenesis. *Front Behav Neurosci*, 14, 96. doi:10.3389/fnbeh.2020.00096

- Kim, K. H., Cho, B. C., Lee, C. G., Kim, H. R., Suh, Y. G., Kim, J. W., Choi, C., Baek, J. G., & Cho, J. (2016). Hippocampus-Sparing Whole-Brain Radiotherapy and Simultaneous Integrated Boost for Multiple Brain Metastases From Lung Adenocarcinoma: Early Response and Dosimetric Evaluation. *Technol Cancer Res Treat*, *15*(1), 122-129. doi:10.1177/1533034614566993
- Kocher, M., Soffiatti, R., Abacioglu, U., Villa, S., Fauchon, F., Baumert, B. G., Fariselli, L., Tzuk-Shina, T., Kortmann, R. D., Carrie, C., Ben Hassel, M., Kouri, M., Valeinis, E., van den Berge, D., Collette, S., Collette, L., & Mueller, R. P. (2011). Adjuvant whole-brain radiotherapy versus observation after radiosurgery or surgical resection of one to three cerebral metastases: results of the EORTC 22952-26001 study. *J Clin Oncol*, *29*(2), 134-141. doi:10.1200/JCO.2010.30.1655
- Kotecha, R., & Hall, M. D. (2020). Impact of radiotherapy dosimetric parameters on neurocognitive function in brain tumor patients. *Neuro Oncol*, *22*(11), 1559-1561. doi:10.1093/neuonc/noaa208
- Kuhn, H. G., Dickinson-Anson, H., & Gage, F. H. (1996). Neurogenesis in the dentate gyrus of the adult rat: age-related decrease of neuronal progenitor proliferation. *J Neurosci*, *16*(6), 2027-2033. Retrieved from <https://www.ncbi.nlm.nih.gov/pubmed/8604047>
- Kundapur, V., Ellchuk, T., Ahmed, S., & Gondi, V. (2015). Risk of hippocampal metastases in small cell lung cancer patients at presentation and after cranial irradiation: a safety profile study for hippocampal sparing during prophylactic or therapeutic cranial irradiation. *Int J Radiat Oncol Biol Phys*, *91*(4), 781-786. doi:10.1016/j.ijrobp.2014.12.026
- Laack, N. N., & Brown, P. D. (2004). Cognitive sequelae of brain radiation in adults. *Semin Oncol*, *31*(5), 702-713. doi:10.1053/j.seminoncol.2004.07.013
- Lai, T. W., Zhang, S., & Wang, Y. T. (2014). Excitotoxicity and stroke: identifying novel targets for neuroprotection. *Prog Neurobiol*, *115*, 157-188. doi:10.1016/j.pneurobio.2013.11.006
- Lancelot, E., & Beal, M. F. (1998). Glutamate toxicity in chronic neurodegenerative disease. *Prog Brain Res*, *116*, 331-347. doi:10.1016/s0079-6123(08)60446-x
- Lee, T. C., Greene-Schloesser, D., Payne, V., Diz, D. I., Hsu, F. C., Kooshki, M., Mustafa, R., Riddle, D. R., Zhao, W., Chan, M. D., & Robbins, M. E. (2012). Chronic administration of the angiotensin-converting enzyme inhibitor, ramipril, prevents fractionated whole-brain irradiation-induced perirhinal cortex-dependent cognitive impairment. *Radiat Res*, *178*(1), 46-56. doi:10.1667/rr2731.1
- Lee, W. H., Cho, H. J., Sonntag, W. E., & Lee, Y. W. (2011). Radiation attenuates physiological angiogenesis by differential expression of VEGF, Ang-1, tie-2 and Ang-2 in rat brain. *Radiat Res*, *176*(6), 753-760. doi:10.1667/rr2647.1
- Lee, W. H., Sonntag, W. E., Mitschelen, M., Yan, H., & Lee, Y. W. (2010). Irradiation induces regionally specific alterations in pro-inflammatory environments in rat brain. *Int J Radiat Biol*, *86*(2), 132-144. doi:10.3109/09553000903419346
- Leroi, I., Brandt, J., Reich, S. G., Lyketsos, C. G., Grill, S., Thompson, R., & Marsh, L. (2004). Randomized placebo-controlled trial of donepezil in cognitive impairment in Parkinson's disease. *Int J Geriatr Psychiatry*, *19*(1), 1-8. doi:10.1002/gps.993
- Li, F. P., Winston, K. R., & Gimbrere, K. (1984). Follow-up of children with brain tumors. *Cancer*, *54*(1), 135-138. doi:10.1002/1097-0142(19840701)54:1<135::aid-cnrc2820540127>3.0.co;2-b
- Li, H., Li, Q., Du, X., Sun, Y., Wang, X., Kroemer, G., Blomgren, K., & Zhu, C. (2011). Lithium-mediated long-term neuroprotection in neonatal rat hypoxia-ischemia is associated with antiinflammatory effects and enhanced proliferation and survival of neural stem/progenitor cells. *J Cereb Blood Flow Metab*, *31*(10), 2106-2115. doi:10.1038/jcbfm.2011.75
- Li, J., Bentzen, S. M., Renschler, M., & Mehta, M. P. (2007). Regression after whole-brain radiation therapy for brain metastases correlates with survival and improved neurocognitive function. *J Clin Oncol*, *25*(10), 1260-1266. doi:10.1200/JCO.2006.09.2536

- Li, J., Feng, L., Xing, Y., Wang, Y., Du, L., Xu, C., Cao, J., Wang, Q., Fan, S., Liu, Q., & Fan, F. (2014). Radioprotective and antioxidant effect of resveratrol in hippocampus by activating Sirt1. *Int J Mol Sci*, *15*(4), 5928-5939. doi:10.3390/ijms15045928
- Li, Q., Li, H., Roughton, K., Wang, X., Kroemer, G., Blomgren, K., & Zhu, C. (2010). Lithium reduces apoptosis and autophagy after neonatal hypoxia-ischemia. *Cell Death Dis*, *1*, e56. doi:10.1038/cddis.2010.33
- Li, Y. Q., Chen, P., Haimovitz-Friedman, A., Reilly, R. M., & Wong, C. S. (2003). Endothelial apoptosis initiates acute blood-brain barrier disruption after ionizing radiation. *Cancer Res*, *63*(18), 5950-5956. Retrieved from <https://www.ncbi.nlm.nih.gov/pubmed/14522921>
- Liu, R., Page, M., Solheim, K., Fox, S., & Chang, S. M. (2009). Quality of life in adults with brain tumors: current knowledge and future directions. *Neuro Oncol*, *11*(3), 330-339. doi:10.1215/15228517-2008-093
- Ljubimova, N. V., Levitman, M. K., Plotnikova, E. D., & Eidus, L. (1991). Endothelial cell population dynamics in rat brain after local irradiation. *Br J Radiol*, *64*(766), 934-940. doi:10.1259/0007-1285-64-766-934
- Locksmith, J. P., & Powers, W. E. (1968). Permanent radiation myelopathy. *Am J Roentgenol Radium Ther Nucl Med*, *102*(4), 916-926. Retrieved from <https://www.ncbi.nlm.nih.gov/pubmed/5643218>
- Madsen, T. M., Kristjansen, P. E., Bolwig, T. G., & Wortwein, G. (2003). Arrested neuronal proliferation and impaired hippocampal function following fractionated brain irradiation in the adult rat. *Neuroscience*, *119*(3), 635-642. doi:10.1016/s0306-4522(03)00199-4
- Malaterre, J., McPherson, C. S., Denoyer, D., Lai, E., Hagekyriakou, J., Lightowler, S., Shudo, K., Ernst, M., Ashley, D. M., Short, J. L., Wheeler, G., & Ramsay, R. G. (2012). Enhanced lithium-induced brain recovery following cranial irradiation is not impeded by inflammation. *Stem Cells Transl Med*, *1*(6), 469-479. doi:10.5966/sctm.2011-0046
- Malouf, R., & Birks, J. (2004). Donepezil for vascular cognitive impairment. *Cochrane Database Syst Rev*(1), CD004395. doi:10.1002/14651858.CD004395.pub2
- Mao, X. W., Favre, C. J., Fike, J. R., Kubinova, L., Anderson, E., Campbell-Beachler, M., Jones, T., Smith, A., Rightnar, S., & Nelson, G. A. (2010). High-LET radiation-induced response of microvessels in the Hippocampus. *Radiat Res*, *173*(4), 486-493. doi:10.1667/RR1728.1
- Massey, P. V., & Bashir, Z. I. (2007). Long-term depression: multiple forms and implications for brain function. *Trends Neurosci*, *30*(4), 176-184. doi:10.1016/j.tins.2007.02.005
- Meyers, C. A., & Brown, P. D. (2006). Role and relevance of neurocognitive assessment in clinical trials of patients with CNS tumors. *J Clin Oncol*, *24*(8), 1305-1309. doi:10.1200/JCO.2005.04.6086
- Meyers, C. A., Smith, J. A., Bezjak, A., Mehta, M. P., Liebmann, J., Illidge, T., Kunkler, I., Caudrelier, J. M., Eisenberg, P. D., Meerwaldt, J., Siemers, R., Carrie, C., Gaspar, L. E., Curran, W., Phan, S. C., Miller, R. A., & Renschler, M. F. (2004). Neurocognitive function and progression in patients with brain metastases treated with whole-brain radiation and motexafin gadolinium: results of a randomized phase III trial. *J Clin Oncol*, *22*(1), 157-165. doi:10.1200/JCO.2004.05.128
- Michaelidesova, A., Konirova, J., Bartunek, P., & Zikova, M. (2019). Effects of Radiation Therapy on Neural Stem Cells. *Genes (Basel)*, *10*(9). doi:10.3390/genes10090640
- Mizumatsu, S., Monje, M. L., Morhardt, D. R., Rola, R., Palmer, T. D., & Fike, J. R. (2003). Extreme sensitivity of adult neurogenesis to low doses of X-irradiation. *Cancer Res*, *63*(14), 4021-4027. Retrieved from <https://www.ncbi.nlm.nih.gov/pubmed/12874001>
- Monje, M. L., Mizumatsu, S., Fike, J. R., & Palmer, T. D. (2002). Irradiation induces neural precursor-cell dysfunction. *Nat Med*, *8*(9), 955-962. doi:10.1038/nm749
- Monje, M. L., Toda, H., & Palmer, T. D. (2003). Inflammatory blockade restores adult hippocampal neurogenesis. *Science*, *302*(5651), 1760-1765. doi:10.1126/science.1088417

- Monje, M. L., Vogel, H., Masek, M., Ligon, K. L., Fisher, P. G., & Palmer, T. D. (2007). Impaired human hippocampal neurogenesis after treatment for central nervous system malignancies. *Ann Neurol*, *62*(5), 515-520. doi:10.1002/ana.21214
- Moulder, J. E., & Cohen, E. P. (2007). Future strategies for mitigation and treatment of chronic radiation-induced normal tissue injury. *Semin Radiat Oncol*, *17*(2), 141-148. doi:10.1016/j.semradonc.2006.11.010
- Mulkey, R. M., & Malenka, R. C. (1992). Mechanisms underlying induction of homosynaptic long-term depression in area CA1 of the hippocampus. *Neuron*, *9*(5), 967-975. doi:10.1016/0896-6273(92)90248-c
- Naseri, S., Moghahi, S., Mokhtari, T., Roghani, M., Shirazi, A. R., Malek, F., & Rastegar, T. (2017). Radio-Protective Effects of Melatonin on Subventricular Zone in Irradiated Rat: Decrease in Apoptosis and Upregulation of Nestin. *J Mol Neurosci*, *63*(2), 198-205. doi:10.1007/s12031-017-0970-5
- Nordal, R. A., Nagy, A., Pintilie, M., & Wong, C. S. (2004). Hypoxia and hypoxia-inducible factor-1 target genes in central nervous system radiation injury: a role for vascular endothelial growth factor. *Clin Cancer Res*, *10*(10), 3342-3353. doi:10.1158/1078-0432.CCR-03-0426
- Oehlke, O., Wucherpennig, D., Fels, F., Frings, L., Egger, K., Weyerbrock, A., Prokic, V., Nieder, C., & Grosu, A. L. (2015). Whole brain irradiation with hippocampal sparing and dose escalation on multiple brain metastases: Local tumour control and survival. *Strahlenther Onkol*, *191*(6), 461-469. doi:10.1007/s00066-014-0808-9
- Orgogozo, J. M., Rigaud, A. S., Stoffler, A., Mobius, H. J., & Forette, F. (2002). Efficacy and safety of memantine in patients with mild to moderate vascular dementia: a randomized, placebo-controlled trial (MMM 300). *Stroke*, *33*(7), 1834-1839. doi:10.1161/01.str.0000020094.08790.49
- Orrego, F., & Villanueva, S. (1993). The chemical nature of the main central excitatory transmitter: a critical appraisal based upon release studies and synaptic vesicle localization. *Neuroscience*, *56*(3), 539-555. doi:10.1016/0306-4522(93)90355-j
- Oskan, F., Ganswindt, U., Schwarz, S. B., Manapov, F., Belka, C., & Niyazi, M. (2014). Hippocampus sparing in whole-brain radiotherapy. A review. *Strahlenther Onkol*, *190*(4), 337-341. doi:10.1007/s00066-013-0518-8
- Packer, R. J., Meadows, A. T., Rorke, L. B., Goldwein, J. L., & D'Angio, G. (1987). Long-term sequelae of cancer treatment on the central nervous system in childhood. *Med Pediatr Oncol*, *15*(5), 241-253. doi:10.1002/mpo.2950150505
- Parihar, V. K., & Limoli, C. L. (2013). Cranial irradiation compromises neuronal architecture in the hippocampus. *Proc Natl Acad Sci U S A*, *110*(31), 12822-12827. doi:10.1073/pnas.1307301110
- Prager, I., Patties, I., Himmelbach, K., Kendzia, E., Merz, F., Muller, K., Kortmann, R. D., & Glasow, A. (2016). Dose-dependent short- and long-term effects of ionizing irradiation on neural stem cells in murine hippocampal tissue cultures: neuroprotective potential of resveratrol. *Brain Behav*, *6*(10), e00548. doi:10.1002/brb3.548
- Prokic, V., Wiedenmann, N., Fels, F., Schmucker, M., Nieder, C., & Grosu, A. L. (2013). Whole brain irradiation with hippocampal sparing and dose escalation on multiple brain metastases: a planning study on treatment concepts. *Int J Radiat Oncol Biol Phys*, *85*(1), 264-270. doi:10.1016/j.ijrobp.2012.02.036
- Raber, J., Allen, A. R., Weber, S., Chakraborti, A., Sharma, S., & Fike, J. R. (2016). Effect of behavioral testing on spine density of basal dendrites in the CA1 region of the hippocampus modulated by (56)Fe irradiation. *Behav Brain Res*, *302*, 263-268. doi:10.1016/j.bbr.2016.01.035
- Raber, J., Rola, R., LeFevour, A., Morhardt, D., Curley, J., Mizumatsu, S., VandenBerg, S. R., & Fike, J. R. (2004). Radiation-induced cognitive impairments are associated with changes in indicators of hippocampal neurogenesis. *Radiat Res*, *162*(1), 39-47. doi:10.1667/rr3206

- Ramanan, S., Kooshki, M., Zhao, W., Hsu, F. C., Riddle, D. R., & Robbins, M. E. (2009). The PPARalpha agonist fenofibrate preserves hippocampal neurogenesis and inhibits microglial activation after whole-brain irradiation. *Int J Radiat Oncol Biol Phys*, *75*(3), 870-877. doi:10.1016/j.ijrobp.2009.06.059
- Ramanan, S., Zhao, W., Riddle, D. R., & Robbins, M. E. (2010). Role of PPARs in Radiation-Induced Brain Injury. *PPAR Res*, *2010*, 234975. doi:10.1155/2010/234975
- Rapp, S. R., Case, L. D., Peiffer, A., Naughton, M. M., Chan, M. D., Stieber, V. W., Moore, D. F., Jr., Falchuk, S. C., Piephoff, J. V., Edenfield, W. J., Giguere, J. K., Loghin, M. E., & Shaw, E. G. (2015). Donepezil for Irradiated Brain Tumor Survivors: A Phase III Randomized Placebo-Controlled Clinical Trial. *J Clin Oncol*, *33*(15), 1653-1659. doi:10.1200/JCO.2014.58.4508
- Redmond, K. J., Mahone, E. M., Terezakis, S., Ishaq, O., Ford, E., McNutt, T., Kleinberg, L., Cohen, K. J., Wharam, M., & Horska, A. (2013). Association between radiation dose to neuronal progenitor cell niches and temporal lobes and performance on neuropsychological testing in children: a prospective study. *Neuro Oncol*, *15*(3), 360-369. doi:10.1093/neuonc/nos303
- Reinhold, H. S., Calvo, W., Hopewell, J. W., & van der Berg, A. P. (1990). Development of blood vessel-related radiation damage in the fimbria of the central nervous system. *Int J Radiat Oncol Biol Phys*, *18*(1), 37-42. doi:10.1016/0360-3016(90)90264-k
- Robbins, M. E., Zhao, W., Garcia-Espinosa, M. A., & Diz, D. I. (2010). Renin-angiotensin system blockers and modulation of radiation-induced brain injury. *Curr Drug Targets*, *11*(11), 1413-1422. doi:10.2174/1389450111009011413
- Robison, L. L., Armstrong, G. T., Boice, J. D., Chow, E. J., Davies, S. M., Donaldson, S. S., Green, D. M., Hammond, S., Meadows, A. T., Mertens, A. C., Mulvihill, J. J., Nathan, P. C., Neglia, J. P., Packer, R. J., Rajaraman, P., Sklar, C. A., Stovall, M., Strong, L. C., Yasui, Y., & Zeltzer, L. K. (2009). The Childhood Cancer Survivor Study: a National Cancer Institute-supported resource for outcome and intervention research. *J Clin Oncol*, *27*(14), 2308-2318. doi:10.1200/JCO.2009.22.3339
- Rola, R., Raber, J., Rizk, A., Otsuka, S., VandenBerg, S. R., Morhardt, D. R., & Fike, J. R. (2004). Radiation-induced impairment of hippocampal neurogenesis is associated with cognitive deficits in young mice. *Exp Neurol*, *188*(2), 316-330. doi:10.1016/j.expneurol.2004.05.005
- Roman, D. D., & Sperduto, P. W. (1995). Neuropsychological effects of cranial radiation: current knowledge and future directions. *Int J Radiat Oncol Biol Phys*, *31*(4), 983-998. doi:10.1016/0360-3016(94)00550-8
- Rosi, S., Andres-Mach, M., Fishman, K. M., Levy, W., Ferguson, R. A., & Fike, J. R. (2008). Cranial irradiation alters the behaviorally induced immediate-early gene arc (activity-regulated cytoskeleton-associated protein). *Cancer Res*, *68*(23), 9763-9770. doi:10.1158/0008-5472.CAN-08-1861
- Roughton, K., Andreasson, U., Blomgren, K., & Kalm, M. (2013). Lipopolysaccharide-induced inflammation aggravates irradiation-induced injury to the young mouse brain. *Dev Neurosci*, *35*(5), 406-415. doi:10.1159/000353820
- Scarpini, E., Scheltens, P., & Feldman, H. (2003). Treatment of Alzheimer's disease: current status and new perspectives. *Lancet Neurol*, *2*(9), 539-547. doi:10.1016/s1474-4422(03)00502-7
- Schindler, M. K., Forbes, M. E., Robbins, M. E., & Riddle, D. R. (2008). Aging-dependent changes in the radiation response of the adult rat brain. *Int J Radiat Oncol Biol Phys*, *70*(3), 826-834. doi:10.1016/j.ijrobp.2007.10.054
- Schmal, Z., Isermann, A., Hladik, D., von Toerne, C., Tapio, S., & Rube, C. E. (2019). DNA damage accumulation during fractionated low-dose radiation compromises hippocampal neurogenesis. *Radiother Oncol*, *137*, 45-54. doi:10.1016/j.radonc.2019.04.021
- Schnegg, C. I., Greene-Schloesser, D., Kooshki, M., Payne, V. S., Hsu, F. C., & Robbins, M. E. (2013). The PPARdelta agonist GW0742 inhibits neuroinflammation, but does not restore neurogenesis or

- prevent early delayed hippocampal-dependent cognitive impairment after whole-brain irradiation. *Free Radic Biol Med*, 61, 1-9. doi:10.1016/j.freeradbiomed.2013.03.002
- Schultheiss, T. E., & Stephens, L. C. (1992). Invited review: permanent radiation myelopathy. *Br J Radiol*, 65(777), 737-753. doi:10.1259/0007-1285-65-777-737
- Seltzer, B. (2007). Donepezil: an update. *Expert Opin Pharmacother*, 8(7), 1011-1023. doi:10.1517/14656566.8.7.1011
- Sener, G., Jahovic, N., Tosun, O., Atasoy, B. M., & Yegen, B. C. (2003). Melatonin ameliorates ionizing radiation-induced oxidative organ damage in rats. *Life Sci*, 74(5), 563-572. doi:10.1016/j.lfs.2003.05.011
- Sheline, G. E., Wara, W. M., & Smith, V. (1980). Therapeutic irradiation and brain injury. *Int J Radiat Oncol Biol Phys*, 6(9), 1215-1228. doi:10.1016/0360-3016(80)90175-3
- Shinohara, C., Gobbel, G. T., Lamborn, K. R., Tada, E., & Fike, J. R. (1997). Apoptosis in the subependyma of young adult rats after single and fractionated doses of X-rays. *Cancer Res*, 57(13), 2694-2702. Retrieved from <https://www.ncbi.nlm.nih.gov/pubmed/9205079>
- Shirai, K., Mizui, T., Suzuki, Y., Okamoto, M., Hanamura, K., Yoshida, Y., Hino, M., Noda, S. E., Al-jahdari, W. S., Chakravarti, A., Shirao, T., & Nakano, T. (2013). X irradiation changes dendritic spine morphology and density through reduction of cytoskeletal proteins in mature neurons. *Radiat Res*, 179(6), 630-636. doi:10.1667/RR3098.1
- Sievert, W., Stangl, S., Steiger, K., & Multhoff, G. (2018). Improved Overall Survival of Mice by Reducing Lung Side Effects After High-Precision Heart Irradiation Using a Small Animal Radiation Research Platform. *Int J Radiat Oncol Biol Phys*, 101(3), 671-679. doi:10.1016/j.ijrobp.2018.02.017
- Simmons, D. A., Lartey, F. M., Schuler, E., Rafat, M., King, G., Kim, A., Ko, R., Semaan, S., Gonzalez, S., Jenkins, M., Pradhan, P., Shih, Z., Wang, J., von Eyben, R., Graves, E. E., Maxim, P. G., Longo, F. M., & Loo, B. W., Jr. (2019). Reduced cognitive deficits after FLASH irradiation of whole mouse brain are associated with less hippocampal dendritic spine loss and neuroinflammation. *Radiother Oncol*, 139, 4-10. doi:10.1016/j.radonc.2019.06.006
- Slotman, B., Faivre-Finn, C., Kramer, G., Rankin, E., Snee, M., Hatton, M., Postmus, P., Collette, L., Musat, E., Senan, S., Group, E. R. O., & Lung Cancer, G. (2007). Prophylactic cranial irradiation in extensive small-cell lung cancer. *N Engl J Med*, 357(7), 664-672. doi:10.1056/NEJMoa071780
- Snyder, J. S., Kee, N., & Wojtowicz, J. M. (2001). Effects of adult neurogenesis on synaptic plasticity in the rat dentate gyrus. *J Neurophysiol*, 85(6), 2423-2431. doi:10.1152/jn.2001.85.6.2423
- Son, Y., Byun, S. J., & Pae, H. O. (2013). Involvement of heme oxygenase-1 expression in neuroprotection by piceatannol, a natural analog and a metabolite of resveratrol, against glutamate-mediated oxidative injury in HT22 neuronal cells. *Amino Acids*, 45(2), 393-401. doi:10.1007/s00726-013-1518-9
- Song, J., Kang, S. M., Lee, K. M., & Lee, J. E. (2015). The protective effect of melatonin on neural stem cell against LPS-induced inflammation. *Biomed Res Int*, 2015, 854359. doi:10.1155/2015/854359
- Stahel, P. F., Smith, W. R., Bruchis, J., & Rabb, C. H. (2008). Peroxisome proliferator-activated receptors: "key" regulators of neuroinflammation after traumatic brain injury. *PPAR Res*, 2008, 538141. doi:10.1155/2008/538141
- Sun, X. Z., Inouye, M., Hayasaka, S., & Yamamura, H. (1994). Body and brain development following exposure to 60Co gamma-irradiation during pregnancy in mice. *Environ Med*, 38(2), 111-114. Retrieved from <https://www.ncbi.nlm.nih.gov/pubmed/12703523>
- Tofilon, P. J., & Fike, J. R. (2000). The radioresponse of the central nervous system: a dynamic process. *Radiat Res*, 153(4), 357-370. doi:10.1667/0033-7587(2000)153[0357:trotcn]2.0.co;2
- Truong, V. L., Jun, M., & Jeong, W. S. (2018). Role of resveratrol in regulation of cellular defense systems against oxidative stress. *Biofactors*, 44(1), 36-49. doi:10.1002/biof.1399

- Tulke, S., Haas, C. A., & Haussler, U. (2019). Expression of brain-derived neurotrophic factor and structural plasticity in the dentate gyrus and CA2 region correlate with epileptiform activity. *Epilepsia*, *60*(6), 1234-1247. doi:10.1111/epi.15540
- Turnquist, C., Beck, J. A., Horikawa, I., Obiorah, I. E., Von Muhlinen, N., Vojtesek, B., Lane, D. P., Grunseich, C., Chahine, J. J., Ames, H. M., Smart, D. D., Harris, B. T., & Harris, C. C. (2019). Radiation-induced astrocyte senescence is rescued by Delta133p53. *Neuro Oncol*, *21*(4), 474-485. doi:10.1093/neuonc/noz001
- Turnquist, C., Harris, B. T., & Harris, C. C. (2020). Radiation-induced brain injury: current concepts and therapeutic strategies targeting neuroinflammation. *Neurooncol Adv*, *2*(1), vdaa057. doi:10.1093/oaajnl/vdaa057
- van Kessel, E., Baumfalk, A. E., van Zandvoort, M. J. E., Robe, P. A., & Snijders, T. J. (2017). Tumor-related neurocognitive dysfunction in patients with diffuse glioma: a systematic review of neurocognitive functioning prior to anti-tumor treatment. *J Neurooncol*, *134*(1), 9-18. doi:10.1007/s11060-017-2503-z
- von Bohlen Und Halbach, O. (2009). Structure and function of dendritic spines within the hippocampus. *Ann Anat*, *191*(6), 518-531. doi:10.1016/j.aanat.2009.08.006
- Walker, A. J., Ruzevick, J., Malayeri, A. A., Rigamonti, D., Lim, M., Redmond, K. J., & Kleinberg, L. (2014). Postradiation imaging changes in the CNS: how can we differentiate between treatment effect and disease progression? *Future Oncol*, *10*(7), 1277-1297. doi:10.2217/fon.13.271
- Wang, Y., Boerma, M., & Zhou, D. (2016). Ionizing Radiation-Induced Endothelial Cell Senescence and Cardiovascular Diseases. *Radiat Res*, *186*(2), 153-161. doi:10.1667/RR14445.1
- Warrington, J. P., Csiszar, A., Johnson, D. A., Herman, T. S., Ahmad, S., Lee, Y. W., & Sonntag, W. E. (2011). Cerebral microvascular rarefaction induced by whole brain radiation is reversible by systemic hypoxia in mice. *Am J Physiol Heart Circ Physiol*, *300*(3), H736-744. doi:10.1152/ajpheart.01024.2010
- Wexler, E. M., Geschwind, D. H., & Palmer, T. D. (2008). Lithium regulates adult hippocampal progenitor development through canonical Wnt pathway activation. *Mol Psychiatry*, *13*(3), 285-292. doi:10.1038/sj.mp.4002093
- Wilcock, G., Mobius, H. J., Stoffler, A., & group, M. M. M. (2002). A double-blind, placebo-controlled multicentre study of memantine in mild to moderate vascular dementia (MMM500). *Int Clin Psychopharmacol*, *17*(6), 297-305. doi:10.1097/00004850-200211000-00005
- Wilke, C., Grosshans, D., Duman, J., Brown, P., & Li, J. (2018). Radiation-induced cognitive toxicity: pathophysiology and interventions to reduce toxicity in adults. *Neuro Oncol*, *20*(5), 597-607. doi:10.1093/neuonc/nox195
- Wilson, J. X. (1997). Antioxidant defense of the brain: a role for astrocytes. *Can J Physiol Pharmacol*, *75*(10-11), 1149-1163. Retrieved from <https://www.ncbi.nlm.nih.gov/pubmed/9431439>
- Witter, M. P., Wouterlood, F. G., Naber, P. A., & Van Haeften, T. (2000). Anatomical organization of the parahippocampal-hippocampal network. *Ann N Y Acad Sci*, *911*, 1-24. doi:10.1111/j.1749-6632.2000.tb06716.x
- Wu, P. H., Coultrap, S., Pinnix, C., Davies, K. D., Tailor, R., Ang, K. K., Browning, M. D., & Grosshans, D. R. (2012). Radiation induces acute alterations in neuronal function. *PLoS One*, *7*(5), e37677. doi:10.1371/journal.pone.0037677
- Yazlovitskaya, E. M., Edwards, E., Thotala, D., Fu, A., Osusky, K. L., Whetsell, W. O., Jr., Boone, B., Shinohara, E. T., & Hallahan, D. E. (2006). Lithium treatment prevents neurocognitive deficit resulting from cranial irradiation. *Cancer Res*, *66*(23), 11179-11186. doi:10.1158/0008-5472.CAN-06-2740
- Zanni, G., Di Martino, E., Omelyanenko, A., Andang, M., Delle, U., Elmroth, K., & Blomgren, K. (2015). Lithium increases proliferation of hippocampal neural stem/progenitor cells and rescues

- irradiation-induced cell cycle arrest in vitro. *Oncotarget*, 6(35), 37083-37097. doi:10.18632/oncotarget.5191
- Zanni, G., Goto, S., Fragopoulou, A. F., Gaudenzi, G., Naidoo, V., Di Martino, E., Levy, G., Dominguez, C. A., Dethlefsen, O., Cedazo-Minguez, A., Merino-Serrais, P., Stamatakis, A., Hermanson, O., & Blomgren, K. (2021). Lithium treatment reverses irradiation-induced changes in rodent neural progenitors and rescues cognition. *Mol Psychiatry*, 26(1), 322-340. doi:10.1038/s41380-019-0584-0
- Zanni, G., Zhou, K., Riebe, I., Xie, C., Zhu, C., Hanse, E., & Blomgren, K. (2015). Irradiation of the Juvenile Brain Provokes a Shift from Long-Term Potentiation to Long-Term Depression. *Dev Neurosci*, 37(3), 263-272. doi:10.1159/000430435
- Zhang, D., Zhou, W., Lam, T. T., Weng, C., Bronk, L., Ma, D., Wang, Q., Duman, J. G., Dougherty, P. M., & Grosshans, D. R. (2018). Radiation induces age-dependent deficits in cortical synaptic plasticity. *Neuro Oncol*, 20(9), 1207-1214. doi:10.1093/neuonc/noy052
- Zhang, L., Plotkin, R. C., Wang, G., Sandel, M. E., & Lee, S. (2004). Cholinergic augmentation with donepezil enhances recovery in short-term memory and sustained attention after traumatic brain injury. *Arch Phys Med Rehabil*, 85(7), 1050-1055. doi:10.1016/j.apmr.2003.10.014
- Zhao, R., Kong, W., Shang, J., Zhe, H., & Wang, Y. Y. (2017). Hippocampal-Sparing Whole-Brain Radiotherapy for Lung Cancer. *Clin Lung Cancer*, 18(2), 127-131. doi:10.1016/j.clcc.2016.09.007
- Zhao, W., Payne, V., Tommasi, E., Diz, D. I., Hsu, F. C., & Robbins, M. E. (2007). Administration of the peroxisomal proliferator-activated receptor gamma agonist pioglitazone during fractionated brain irradiation prevents radiation-induced cognitive impairment. *Int J Radiat Oncol Biol Phys*, 67(1), 6-9. doi:10.1016/j.ijrobp.2006.09.036

7. Appendix

Declaration

Some part of the result and discussion section is modified from the paper “Partial-brain radiation-induced microvascular cognitive impairment in juvenile murine unilateral hippocampal synaptic plasticity” (PMID: 34619330). I am the first and co-corresponding author of this paper.

8. Acknowledgements

My deepest gratitude goes first and foremost to Professor Dr. Gabriele Multhoff, my Doktormutter, for her constant encouragement and patient support which walked me through all the stages of my doctoral research career. I gratefully appreciate her valuable and instructive advices. As time goes by, only her scientific research enthusiasm and the spirit of exploration in my memory will never fade out. The old Chinese saying goes "Always respect your teacher as you do your father", which is also the real reflection of "Doktormutter" for her. It was a great privilege and honor to work and study under her guidance, I feel deeply about this in a foreign country. I am extremely grateful for what she has offered me, I am extending my heartfelt thanks for her care, empathy, and forgiveness.

My sincere thanks also goes to my mentor, Dr. Wolfgang Sievert, for offering me the animal experiment operation opportunities and leading me working on diverse exciting projects. Thanks for his excellent care and suggestions with his warmth and friendliness.

I would like to say thanks to my friends and all research colleagues, especially the whole AG Multhoff group for the pleasant working environment. It was an unforgettable pleasure time spending with you. Thanks to Dr. Stefan Stangl, Dr. Maxim Shevtsov, Dr. Ali Bashiri, Anett Lange, Caro Werner, Melissa Schwab, Marija Pieper, Alicia Hernandez, Mathias Pilz, Arnö Sophia, Hannah Zanth, Fei Wang and Zhiyuan Wu for giving generously help on my experiments.

I would like to thank Prof. Dr. Gerhard Rammes and Dr. Selina Keppler for excellent suggestions. Many thanks to Xènia Puig Bosch and Julian Hofmann for the collaboration.

I would like to thank the China scholarship council for the financial support in Germany.

For my dearest, darling, treasured, cherished Miss Siyan Li whom I worship. With respect, adoration, admiration, kisses, gratitude, best wishes and love for you. Thanks for your patience and understanding during the time period.

Last but not least, my thanks would go to my beloved family for their loving considerations and great confidence in me all through these years. I am thankful for all the good things I have met in my life, even the beauty of passing by, even if it was fleeting.

Munich, 15th of April 2021

9. Curriculum Vitae

Hengyi Fan, born on the 2nd of May 1992 in Linchuan, Jiangxi, P.R.China

Education

- | | |
|-----------------|---|
| 10/2018-Now | Doctoral candidate, Department Radiation Oncology,
Technische Universität München, Germany |
| 09/2015-07/2018 | Master degree, Department of Neurosurgery, Medical
College of Nanchang University, China |
| 09/2010-07/2015 | Bachelor degree, Clinical Medicine, Chengde Medical
University, China |

Clinical experiences

- | | |
|-----------------|--|
| 09/2015-07/2018 | Resident, The Second Affiliated Hospital of Nanchang |
| 01/2014-07/2015 | Medical Intern, Chaoyang Central Hospital |

Scholarships and Awards

Scholarship of China Scholarship Council

China National Scholarship for Master 2017

Publications

1. **Hengyi F[#]**, Wolfgang S, Julian H, Selina J. K, Katja S, Xènia P, Gerhard R, Gabriele M[#]. (2021). Partial-brain radiation-induced microvascular cognitive impairment in juvenile murine unilateral hippocampal synaptic plasticity. *Int J Radiat Oncol Biol Phys*. doi:10.1016/j.ijrobp.2021.09.041. (Co-corresponding author)
2. Lobinger D, Gempt J, Sievert W, Melanie B, Sven S, Huyen N, Stefan S, Caroline W, Fei W, Zhiyuan W, **Hengyi F**, Hannah Z, Maxim S, Mathias P, Isabelle R, Melissa S, Jürgen S, Gabriele M. Potential Role of Hsp70 and Activated NK Cells for Prediction of Prognosis in Glioblastoma Patients. *Front Mol Biosci*. 2021;8:669366. doi:10.3389/fmolb.2021.669366.
3. **Fan H***, Yuan R*, Cheng S*, Xiong K, Zhu X and Zhang Y. Overexpressed miR-183 promoted glioblastoma radioresistance via down-regulating LRIG1. *Biomed Pharmacother*. 2018;97:1554-1563. (Co-first author)
4. Yuan R*, **Fan H***, Cheng S, Gao W, Xu X, Lv S, Ye M, Wu M, Zhu X and Zhang Y. Silymarin prevents NLRP3 inflammasome activation and protects against intracerebral hemorrhage. *Biomed Pharmacother*. 2017;93:308-315. (Co-first author)
5. Cheng SQ*, **Fan HY***, Xu X, Gao WW, Lv SG, Ye MH, Wu MJ, Shen XL, Cheng ZJ, Zhu XG and Zhang Y. Over-expression of LRIG1 suppresses biological function of pituitary adenoma via attenuation of PI3K/AKT and Ras/Raf/ERK pathways in vivo and in vitro. *J Huazhong Univ Sci Technolog Med Sci*. 2016;36:558-563. (Co-first author)
6. Cheng S*, Gao W*, Xu X, **Fan H**, Wu Y, Li F, Zhang J, Zhu X and Zhang Y. Methylprednisolone sodium succinate reduces BBB disruption and inflammation in a model mouse of intracranial haemorrhage. *Brain Res Bull*. 2016;127:226-233.

7. Fan YH*, Ji CX*, Xu B, **Fan HY**, Cheng ZJ and Zhu XG. Long noncoding RNA activated by TGF-beta in human cancers: A meta-analysis. *Clin Chim Acta*. 2017;468:10-16.